PDK1-mediated activation of MRCKα regulates directional cell migration and lamellipodia retraction

Paolo Armando Gagliardi,[1,3] Laura di Blasio,[1,3] Alberto Puliafito,[1,3] Giorgio Seano,[1,3] Roberto Sessa,[1,3] Federica Chianale,[1,3] Thomas Leung,[4] Federico Bussolino,[1,2,3] and Luca Primo[1,2,3]

[1]Department of Oncology and [2]Center for Molecular Systems Biology, University of Turin, Turin 10060, Italy
[3]Laboratory of Cell Migration, Candiolo Cancer Institute FPO-IRCCS, Candiolo 10060, Italy
[4]Institute of Molecular and Cell Biology, A-STAR, Singapore 138673, Singapore

Directional cell migration is of paramount importance in both physiological and pathological processes, such as development, wound healing, immune response, and cancer invasion. Here, we report that 3-phosphoinositide-dependent kinase 1 (PDK1) regulates epithelial directional migration and invasion by binding and activating myotonic dystrophy kinase–related CDC42-binding kinase α (MRCKα). We show that the effect of PDK1 on cell migration does not involve its kinase activity but instead relies on its ability to bind membrane phosphatidylinositol (3,4,5)-trisphosphate. Upon epidermal growth factor (EGF) stimulation, PDK1 and MRCKα colocalize at the cell membrane in lamellipodia. We demonstrate that PDK1 positively modulates MRCKα activity and drives its localization within lamellipodia. Likewise, the retraction phase of lamellipodia is controlled by PDK1 through an MRCKα-dependent mechanism. In summary, we discovered a functional pathway involving PDK1-mediated activation of MRCKα, which links EGF signaling to myosin contraction and directional migration.

Introduction

Directional cell migration is of paramount importance in both physiological and pathological processes, such as wound healing and tumor metastasis (Yamaguchi et al., 2005). Among the different types of directed cell migration, chemotaxis, i.e., migration toward a soluble chemotactic agent, is probably the most studied (Roussos et al., 2011). Because of its ability to bind to phosphatidylinositol (3,4,5)-trisphosphate (PIP3) produced at the leading edge, 3-phosphoinositide–dependent kinase 1 (PDK1) has been recognized as a key regulator of cell migration and chemotaxis. Its role in this process was proved in different cell types and organisms including endothelial cells (Primo et al., 2007), smooth muscle cells (Weber et al., 2004), T lymphocytes (Waugh et al., 2009), neutrophils (Yagi et al., 2009), and *Dictyostelium discoideum* (Liao et al., 2010). PDK1 is a serine/threonine kinase that phosphorylates residues in the activation segment of AGC (cAMP-dependent protein kinase A, cGMP-dependent protein kinase G, and phospholipid-dependent protein kinase C) family proteins (Alessi et al., 1997; Pearce et al., 2010). PDK1 recognizes phosphoinositides phosphorylated in position 3 by phosphatidylinositol 3 kinase (PI3K), through its C-terminal pleckstrin homology (PH) domain. This event localizes PDK1 to the plasma membrane, where it phosphorylates Akt (Currie et al., 1999). PDK1 substrates lacking the PH domain, such as p70S6K, SGK, RSK, and PKC isoforms (Toker and Newton, 2000), require a different mechanism for their activation. In this case, PDK1 binds the hydrophobic motif (HM) on these substrates through its PDK1-interacting fragment (PIF)-binding pocket, leading to their phosphorylation and full activation (Biondi et al., 2001).

Different mechanisms have been proposed to explain the role of PDK1 in cell migration. The concomitant localization of PDK1 and Akt at the cellular leading edge is essential for endothelial cell chemotaxis and angiogenesis (Primo et al., 2007).

Correspondence to Luca Primo: luca.primo@ircc.it

Abbreviations used in this paper: FMI, forward migration index; HGF, hepatocyte growth factor; HM, hydrophobic motif; MLC2, myosin regulatory light chain 2; MRCK, myotonic dystrophy kinase–related CDC42-binding kinase; MyPT1, myosin phosphatase target subunit 1; PDK1, 3-phosphoinositide–dependent kinase 1; PH, pleckstrin homology; PI3K, phosphatidylinositol 3 kinase; PIF, PDK1-interacting fragment; PIP3, phosphatidylinositol (3,4,5)-trisphosphate; PLA, proximity ligation assay; ROCK, Rho-associated protein kinase; TIRF, total internal reflection fluorescence; WT, wild type.

The Rockefeller University Press $30.00
J. Cell Biol. Vol. 206 No. 3 415–433
www.jcb.org/cgi/doi/10.1083/jcb.201312090

Moreover, PDK1 has been shown to regulate cell invasion, in particular of breast cancer and melanoma cells through the activation of PLCγ1 (Raimondi et al., 2012). It has also been reported that PDK1 can control cancer cell motility by regulating cortical acto-myosin contraction in a mechanism involving activation of ROCK1 (Pinner and Sahai, 2008).

Regulation of nonmuscle-myosin activity is essential in directional migration, as well as in multiple cellular processes (Vicente-Manzanares et al., 2009). As regulators of nonmuscle-myosin activity, Rho-activated protein kinases are pivotal regulators of cell migration and tumor cell invasion. This group of kinases belongs to AGC family protein and includes two isoforms of Rho-associated protein kinase (ROCK; Amano et al., 1996)—citron Rho-interacting kinase (CRIK; Di Cunto et al., 1998) and myotonin protein kinase (DMPK; Kaliman and Llagostera, 2008)—and three isoforms of myotonic dystrophy kinase–related CDC42-binding kinase (MRCK; Leung et al., 1998). All these kinases share the ability to increase myosin regulatory light chain 2 (MLC2) phosphorylation either directly, by phosphorylating it on T18 or S19 (Amano et al., 1996), or indirectly, by the phosphorylation of myosin phosphatase target subunit 1 (MyPT1), which results in a further increase of MLC2 phosphorylation (Kimura et al., 1996; Tan et al., 2001a). Phosphorylation of MLC2 results in actomyosin contractility (Ikebe and Hartshorne, 1985).

In contrast to the closely related ROCK kinases that are regulated by the Rho GTPase (Amano et al., 1999), there is relatively little information about MRCKα, MRCKβ, and MRCKγ (Zhao and Manser, 2005). MRCK kinases are downstream effectors of GTPase-CDC42 that play key roles in actin-myosin regulation. The current model of MRCK activation also involves diacylglycerol binding, thereby allowing transautophosphorylation upon appropriate N-terminal interactions. Phosphorylation within the activation loop and the HM provides the means for activation, as demonstrated by the mutation T403A in HM, which completely abolishes MRCK kinase activity (Leung et al., 1998; Tan et al., 2001b).

Here, we show that PDK1 regulates directional migration of breast epithelial cells in a kinase-independent manner by inducing MRCKα activation, myosin phosphorylation, and lamellipodia contraction.

Results

PDK1 regulates directional cell migration

EGF is known to be a potent stimulator of cell migration (Blay and Brown, 1985). The nontransformed mammary epithelial cells MCF10A responded to gradients of EGF in a dose-dependent manner (Fig. S1 A), but in the absence of gradient, EGF was unable to induce a significant increase of migrated cells compared with unstimulated cells (Fig. S1 B). PI3K activity, which plays a crucial role in the EGF signaling pathway (Price et al., 1999), has been demonstrated to be a key regulator of the leading edge in migrating cells (Merlot and Firtel, 2003) and, accordingly, inhibition of PI3K activity resulted in the impairment of MCF10A chemotaxis toward EGF (Fig. S1 C) without affecting their viability at the same concentrations (Fig. S1 D).

Among PI3K downstream effectors potentially involved in directional cell migration, PDK1 has been reported to be required for amoeboid and mesenchymal motility (Primo et al., 2007; Pinner and Sahai, 2008).

To investigate its role in EGF-induced chemotaxis, we stably silenced PDK1 with two different shRNAs transduced by lentiviral vectors (shPDK1 #79 and shPDK1 #81), which were able to efficiently reduce PDK1 protein expression compared with nontargeting control, shScr (Fig. 1 A). PDK1 silencing had a profound effect on chemotaxis in transwell assays at 5 ng/ml EGF, whereas it minimally influenced the still low cell motility in the absence of EGF or when the EGF gradient was abrogated by adding the growth factor in the upper chamber (Fig. 1 A). Moreover, PDK1 knockdown had only marginal effects on cell viability (Fig. S1 E), which is consistent with previous studies (Primo et al., 2007; Liu et al., 2009; Gagliardi et al., 2012). Notably, PDK1 wild-type (PDK1_WT) overexpression (Fig. 1 B) was able to significantly increase chemotaxis toward the gradient of EGF but not cell motility in the presence of a homogenous concentration of EGF (Fig. 1 B). The increased number of migrated cells was not caused by increased cell viability (Fig. S1 F).

To assess PDK1 involvement in directional migration, we tracked single MCF10A cells in a scratch wound healing assay and in a sparse cells motility assay (Fig. 1, C and F; and Videos 1 and 2). In a wound assay, cells moving collectively showed an increased directionality compared with those moving as sparse cells (Fig. 1, C and F). The directionality was quantified by calculating the persistence (Fig. 1, E and H), the ability of a cell to maintain its direction of migration, and the forward migration index (FMI), a parameter that quantifies how much cells are able to migrate in the same direction (Fig. 1, D and G).

PDK1-silenced cells showed a significantly reduced FMI (Fig. 1 D) and persistence (Fig. 1 E) in a wound assay compared with control cells. In contrast, PDK1-silenced sparse cells displayed the same directionality of control cells. Concordantly, PDK1_WT overexpression increased both FMI (Fig. 1 G) and persistence (Fig. 1 H) of wounded cells, but was not able to modify persistence of sparse cells (Fig. 1 H). To exclude off-target effects of shRNA used to silence PDK1, we transduced shPDK1 #79 cells with a PDK1_WT cDNA resistant to silencing (Fig. S1 G). PDK1_WT reexpression completely rescued the migration ability toward EGF (Fig. S1 H), as well as FMI and cell persistence in wound healing assays (Fig. S1, I and J).

The kinase activity of PDK1 is not required for directional migration

To understand the molecular mechanism activated by PDK1 during cell migration, we investigated which domain of PDK1 is required for this function. MCF10A cells were transduced with lentiviral vectors expressing different PDK1 mutants: PDK1_WT, K111N mutant, which abolishes kinase activity (PDK1_KD); PH domain point mutant, which impedes the binding to PIP3 at the membrane (PDK1_K465E); L155E mutant, which prevents the binding to the HM on PDK1 substrates (PDK1_L155E); PH domain-deleted mutant (PDK1_ΔPH); the deletion mutant covering the 50 N-terminal amino acids that bind to Ral-GEF (PDK1_Δ50); and the double points mutant in both PH domain and

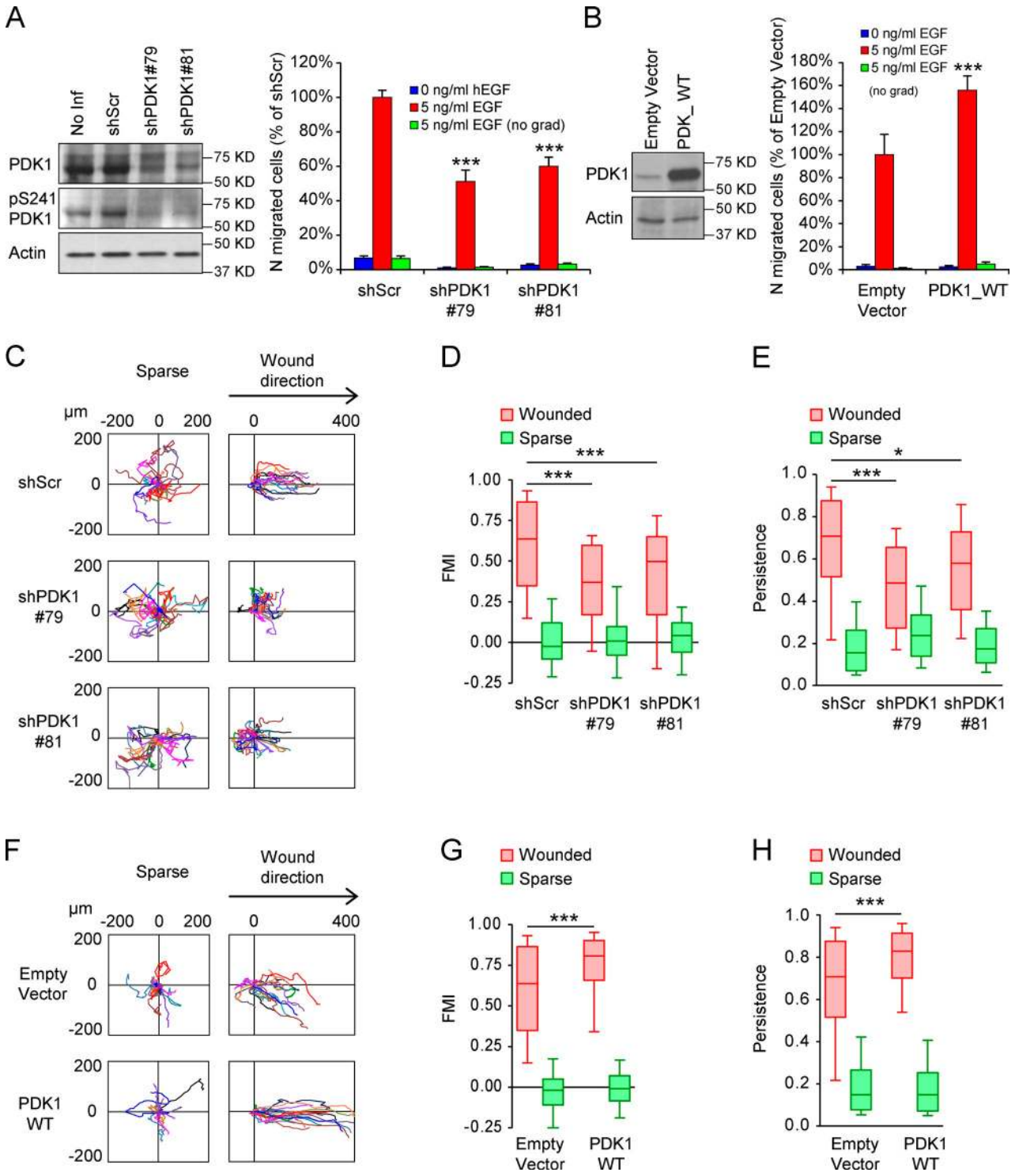

Figure 1. **PDK1 regulates EGF-induced chemotaxis and directional migration of MCF10A cells.** (A) MCF10A cells, infected with lentiviral vectors coding for a control shRNA (shScr) or for shRNAs silencing PDK1 (shPDK1 #79 and shPDK1 #81), were assayed for their migratory ability in the absence of EGF (0 ng/ml EGF), in the presence of 5 ng/ml EGF, or in the presence of 5 ng/ml EGF in both the culture well and in the insert (5 ng/ml EGF [no grad]). PDK1 silencing was verified by immunoblotting. (B) MCF10A cells were infected with a lentiviral vector overexpressing PDK1_WT compared with an empty vector and tested for PDK1 expression and cell migration. Each bar represents the mean and standard error of the mean of three independent experiments. (C) MCF10A shScr, shPDK1 #79, and shPDK1 #81 were cultured as a confluent monolayer and wounded or cultured as sparse cells. Cell movement was tracked and plotted by setting the starting value as 0 µm for both the x and y axes. (D and E) The FMI (D) and persistence (E) of >60 cells was calculated as described in the Materials and methods section. (F–H) MCF10A empty vector or PDK1_WT were tracked upon confluent monolayer wounding or during sparse cell movement (F) and their FMI (G) and persistence (H) were calculated. FMI and persistence were represented as a box plot distribution of >100 cells in three independent experiments. *, $P < 0.05$; **, $P < 0.01$; ***, $P < 0.001$.

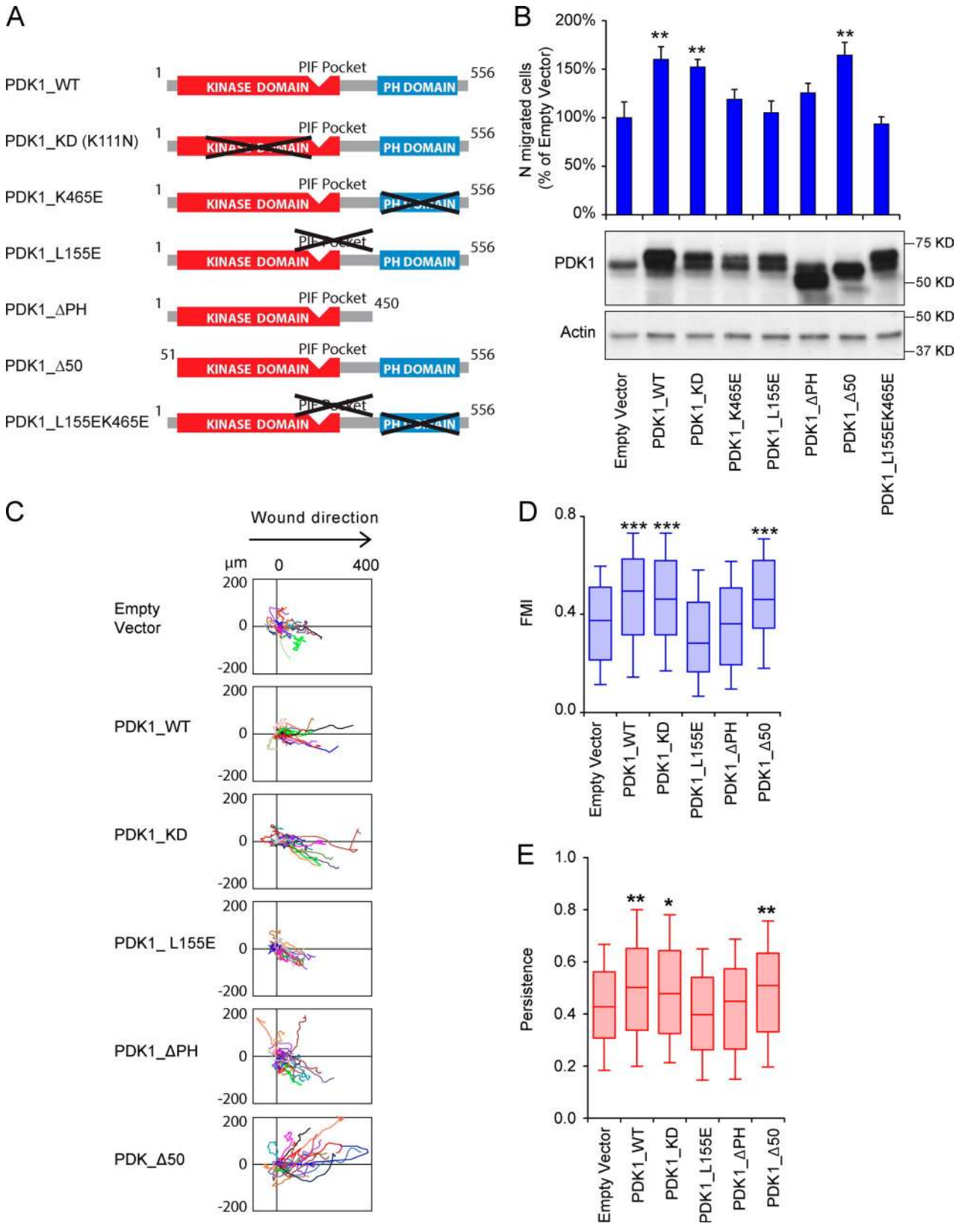

Figure 2. **PDK1 controls cell migration through its PIF-binding pocket and PH domain in a kinase-independent manner.** (A) Schematic structure of PDK1_WT and its functional mutants: PDK1_KD (kinase dead, K111N), PDK1_K465E (point mutation that impairs the ability of the PH domain to bind PIP3), PDK1_L155E (point mutation in the PIF-binding pocket of PDK1 that abrogates the binding to the HM of its substrates), PDK1_ΔPH (lacking the PH domain, amino acids from 451 to 556), PDK1_Δ50 (lacking amino acids from 1 to 50), and PDK1_ K465EL155E (which harbors point mutations of both the PIF-binding pocket and PH domain). (B) MCF10A, transduced with lentiviral vectors coding for PDK1 functional mutants, were assayed for the migration toward 5 ng/ml EGF in comparison to empty vector–transduced cells. PDK1 mutant expression was checked by immunoblotting. Each error bar represents the

PIF-binding pocket (PDK1_L155EK465E; Fig. 2 A). As shown in Fig. 1 B, PDK1_WT overexpression induced an increased migratory ability toward EGF (Fig. 2 B). Surprisingly, PDK1_KD cells had a phenotype comparable to that of PDK1_WT, which suggests that the kinase activity is not necessary to induce cell migration. Similar results were obtained with PDK1_Δ50 mutant. In contrast, PDK1_L155E mutant completely abolished the increase of chemotaxis. The inability to bind membrane-associated PIP3 reduced, but did not completely abrogate, the induction of migration, as shown by PDK1_ΔPH and PDK1_K465E mutants, whereas it was completely prevented by the double mutation of PDK1_L155EK465E (Fig. 2 B).

To exclude the formation of heterodimers between exogenous mutants and endogenous PDK1, which could alter the promoting effect on cell migration, we measured cell migration in the presence of PDK1 mutants expressed in PDK1-silenced cells. Even in these conditions, the expression of either PDK1_WT or PDK1_KD was able to increase cell migration by rescuing the effects of PDK1 silencing (Fig. S2 A). In contrast, both PDK1_ΔPH and PDK1_L155E mutants were unable to rescue the migratory ability of PDK1-silenced cells (Fig. S2 A).

Similar results were obtained in a wound healing assay (Fig. 2 C). Indeed, PDK1_WT, PDK1_KD, and PDK1_Δ50 mutants were able to increase the FMI (Fig. 2 D) and the persistence (Fig. 2 E). In contrast PDK1_ΔPH and PDK1_L155E mutants did not increase FMI or persistence compared with cells transduced with empty vector. To further confirm that the kinase activity of PDK1 is dispensable for the regulation of chemotaxis, we used the specific PDK1 inhibitor GSK2334470, which has been reported to effectively inhibit PDK1 phosphorylation of SGK2, S6K, Akt, and RSK2 at low concentrations (1–3 μM; Najafov et al., 2011; Fig. S2 B). Despite this, GSK2334470 completely failed to block MCF10A chemotaxis toward EGF even at 10 μM (Fig. S2 C), a concentration that caused a significant reduction of cell viability (Fig. S2 D).

MRCKα mediates PDK1-induced directional cell migration

Because the PDK1 effect on cell migration requires the integrity of its PIF-binding pocket but not of the kinase domain, we searched for proteins with a putative PIF sequence, even though they did not contain PDK1 phosphorylatable motifs (Tables S1 and S2). The members of the Rho-GTPase–associated kinase family fulfilled these requirements because, though they lack a classical activation loop consensus motif, they exhibited an HM consensus sequence for the interaction with PDK1. The common function of all Rho-GTPase–associated kinases is the activation of nonmuscular myosin (Zhao and Manser, 2005). Therefore, we evaluated whether MCF10A motility was dependent on the regulation of myosin activity using Blebbistatin, an inhibitor of myosin-II ATPase activity (Limouze et al., 2004; Wilkinson et al., 2005). Treatment with Blebbistatin was able to inhibit both cell migration (Fig. 3 A) and FMI (Fig. 3 D) at concentrations reported to be effective in the inhibition of myosin activity and cell migration in other cell lines (Wilkinson et al., 2005). Thus, we examined the role of Rho-GTPase–associated kinase in this process using specific kinase inhibitors. Unexpectedly, we found that the ROCK inhibitor Y-27632 (Uehata et al., 1997) increased MCF10A migration toward EGF (Fig. 3 B) and FMI (Fig. 3 E). In contrast, the MRCK inhibitor chelerythrine chloride (Tan et al., 2011) completely blocked MCF10A directional migration (Fig. 3 C) and FMI (Fig. 3 F). To confirm the role of MRCK in directional cell migration, we silenced α and β isoforms of MRCK, which are both expressed in MCF10A (Fig. 3 G). Knocking down a single MRCK isoform was not sufficient to recapitulate the effects of an MRCK inhibitor. However, the simultaneous down-regulation of MRCKα and MRCKβ resulted in a significant impairment of cell migration (Fig. S2 E). To understand which MRCK isoform was involved in the PDK1-induced migration, we silenced MRCKα or MRCKβ in MCF10A cells overexpressing PDK1_WT or PDK1_KD (Fig. 3 G). Cell migration experiments showed that MRCKα was required for PDK1 regulation of cell migration, whereas MRCKβ appeared to be dispensable (Fig. 3 H). However, because MRCKβ silencing increased the expression of MRCKα, we could not exclude a compensatory effect (Fig. 3 G). Similarly, silencing of MRCKα, but not MRCKβ, cancelled the increase of FMI (Fig. 3 I) obtained by PDK1_WT and PDK1_KD overexpression. To further exclude the role of ROCK in mediating PDK1 effects, as previously described in amoeboid migration (Pinner and Sahai, 2008), we silenced ROCK1 in MCF10A cells (Fig. 3 J). Down-regulation of ROCK1 failed to reduce the effects of PDK1_WT and PDK1_KD overexpression on both cell migration and FMI (Fig. 3, K and L).

Remarkably, PDK1 played a relevant role in cell migration even in the presence of growth factors other than EGF. In a gradient of hepatocyte growth factor (HGF), MCF10A cells, transduced with control vector, efficiently migrated, whereas PDK1-silenced cells completely lost this ability (Fig. S2 F). The overexpression of PDK1_WT or PDK1_KD strongly increased the number of cells that migrated toward HGF (Fig. S2 G), and this effect is completely dependent on MRCKα (Fig. S2 H).

PDK1 PIF-binding pocket and MRCKα HM mediate the interaction of PDK1 with MRCKα

MRCKα, similar to other AGC kinases, has a highly conserved HM, which is the potential binding site for PDK1. This site is phosphorylated and required for MRCKα activity (Tan et al., 2001b). We hypothesized that PDK1 could associate with MRCKα through the interaction of PDK1 PIF-binding pocket with HM of MRCKα. Consistent with our hypothesis, MRCKα

mean and standard error of the mean of 10 independent experiments. (C) MCF10A cells overexpressing PDK1_WT, PDK1_KD, PDK1_L155E, PDK1_ΔPH, and PDK1_Δ50 or infected with the empty vector were tracked during the wound healing assay. (D and E) Effects of PDK1 mutants overexpression on the FMI (D) and persistence (E). FMI and persistence are represented as box plot distribution of >100 cells in three independent experiments. *, $P < 0.05$; **, $P < 0.01$; ***, $P < 0.001$.

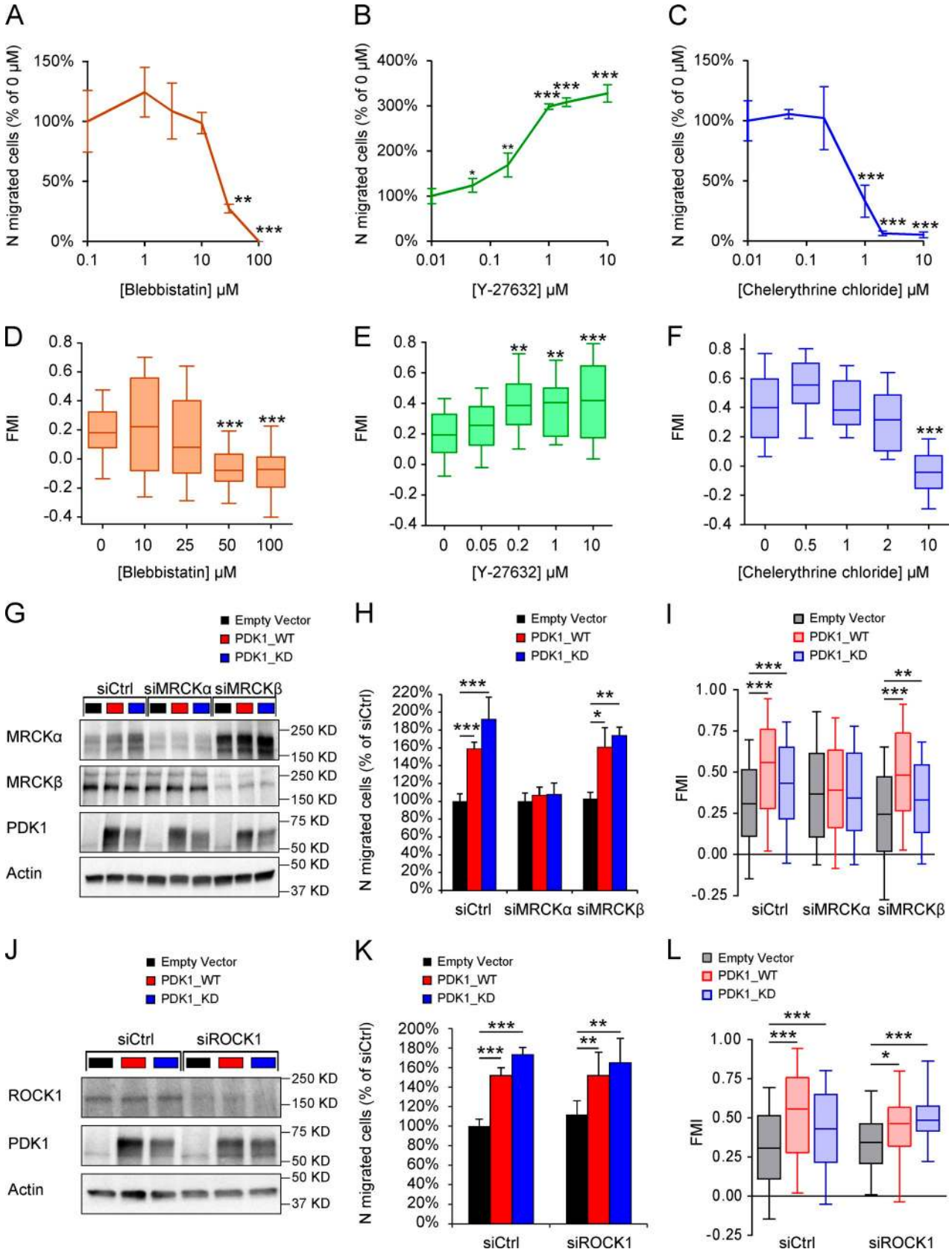

Figure 3. **MRCKα mediates PDK1-induced cell migration.** (A–C) MCF10A cells were tested for their migratory ability toward 5 ng/ml EGF in the presence of increasing concentrations of the inhibitor of nonmuscle myosin II Blebbistatin (A), the ROCK inhibitor Y-27632 (B), or the MRCK inhibitor chelerythrine chloride (C). (D–F) FMI of cells migrating in wound healing in the presence of increasing concentration of Blebbistatin (D), Y-27632 (E), or chelerythrine chloride (F). (G–I) MCF10A cells, stably transduced with lentiviral vectors coding for PDK1_WT or PDK1_KD, compared with an empty vector and transfected with siRNAs targeting, respectively, MRCKα, MRCKβ, or nontargeting (siCtrl), were assayed for PDK1, MRCKα, and MRCKβ protein expression (G), their

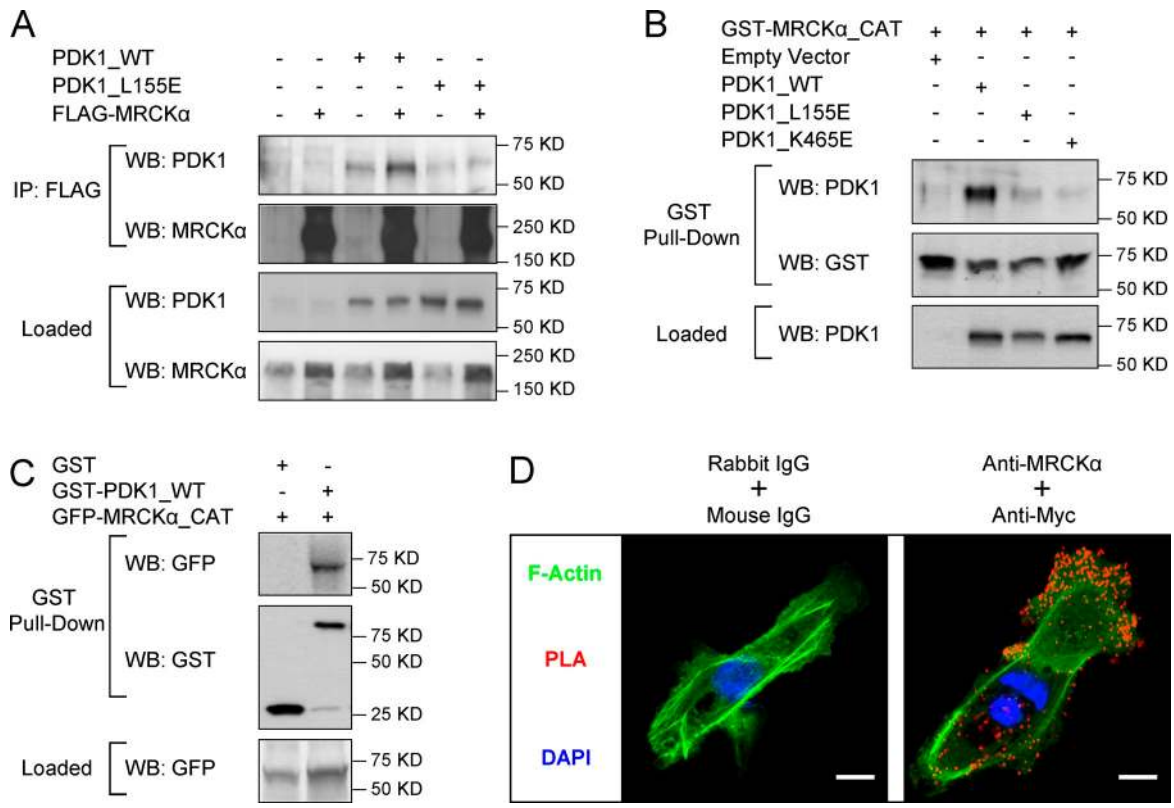

Figure 4. **PDK1 interacts with MRCKα through the PIF-binding pocket.** (A) HeLa cells were stably transduced with lentivirus coding for PDK1_WT, PDK1_L155E, or an empty vector and then transfected with a plasmid driving Flag-MRCKα expression. Immunoprecipitation was performed using an anti-flag antibody. Immunoprecipitated PDK1 was detected by Western blotting. (B) GST-fused MRCKα catalytic subunit (GST-MRCKα_CAT) was purified from 293T cells and used to pull down PDK1 from lysates of MCF10A stably transduced with lentiviral vectors coding for PDK1_WT, PDK1_L155E, PDK1_K465E, or an empty vector. Pulled-down PDK1 was detected by immunoblotting. (C) GST-PDK1_WT was produced and purified from 293T and used to pull down GFP-MRCKα_CAT. Pulled-down GFP-MRCKα_CAT was detected by immunoblotting. (D) MCF10A cells were infected with a lentivirus coding for myc-PDK1 and, after EGF deprivation, stimulated for 200 s with EGF 5 ng/ml. PLA of myc-PDK1 and MRCKα was performed using as detecting antibodies anti–c-Myc produced in mouse and anti-MRCKα produced in rabbit or with the combination of unspecific immunoglobulins (IgG M and IgG R). Cellular shape was identified by Phalloidin-488 staining. Bar, 10 µm.

was able to coimmunoprecipitate PDK1_WT, but not PDK1_L155E (Fig. 4 A). Moreover, we performed a pull-down assay with the recombinant catalytic domain (CAT) of MRCKα, which contains the HM, to confirm that the PIF-binding pocket of PDK1 is involved in the interaction with MRCKα. As expected, L155E mutation abolished the binding of PDK1 with MRCKα (Fig. 4 B). In addition, we assayed the interaction of MRCKα_CAT with the PDK1_K465E mutant, which is unable to bind PIP3 produced by PI3K. This mutation also prevented the binding between PDK1 and MRCKα catalytic domain (Fig. 4 B). Pull-down experiments with the recombinant catalytic domain of MRCKβ, which holds a conserved HM highly similar to that of MRCKα, showed that PDK1 also associates with MRCKβ (Fig. S3 A).

To further confirm the direct interaction of PDK1 with MRCKα, we performed the reverse pull-down with GST-PDK1. In this case as well, GST-PDK1_WT was able to efficiently pull-down GFP-MRCKα_CAT (Fig. 4 C).

The interaction of PDK1 with MRCKα was also analyzed in intact cells by performing in situ proximity ligation assay (PLA) experiments. Myc-tagged PDK1 and endogenous MRCKα, detected with their respective antibodies, showed fluorescent spots, indicative of their proximity localization, whereas nonimmune Ig did not display any fluorescence signal (Fig. 4 D).

PDK1 regulates MRCKα kinase activity

The main biochemical function of MRCKα is the activation of nonmuscular myosin, either directly by phosphorylation of MLC2 or indirectly through inactivation of the MyPT1 by phosphorylation of T696 residue (Tan et al., 2001a). The need for MRCKα in PDK1-induced migration prompted us to investigate

migratory ability toward 5 ng/ml EGF (H), or for the directional migration in wound healing (I). (J–L) MCF10A empty vector, PDK1_WT, or PDK1_KD, transfected with siRNAs targeting ROCK1 or nontargeting (siCtrl), were assayed for PDK1 and ROCK1 protein expression (J), their migratory ability toward 5 ng/ml EGF (K), or for the directional migration in a wound healing assay (L). Each bar in A, B, C, H, and K represents the mean and standard error of the mean of seven independent experiments. In D, E, F, I, and L, data are represented as box plot distributions of >100 cells and were obtained from three independent experiments. *, $P < 0.05$; **, $P < 0.01$; ***, $P < 0.001$.

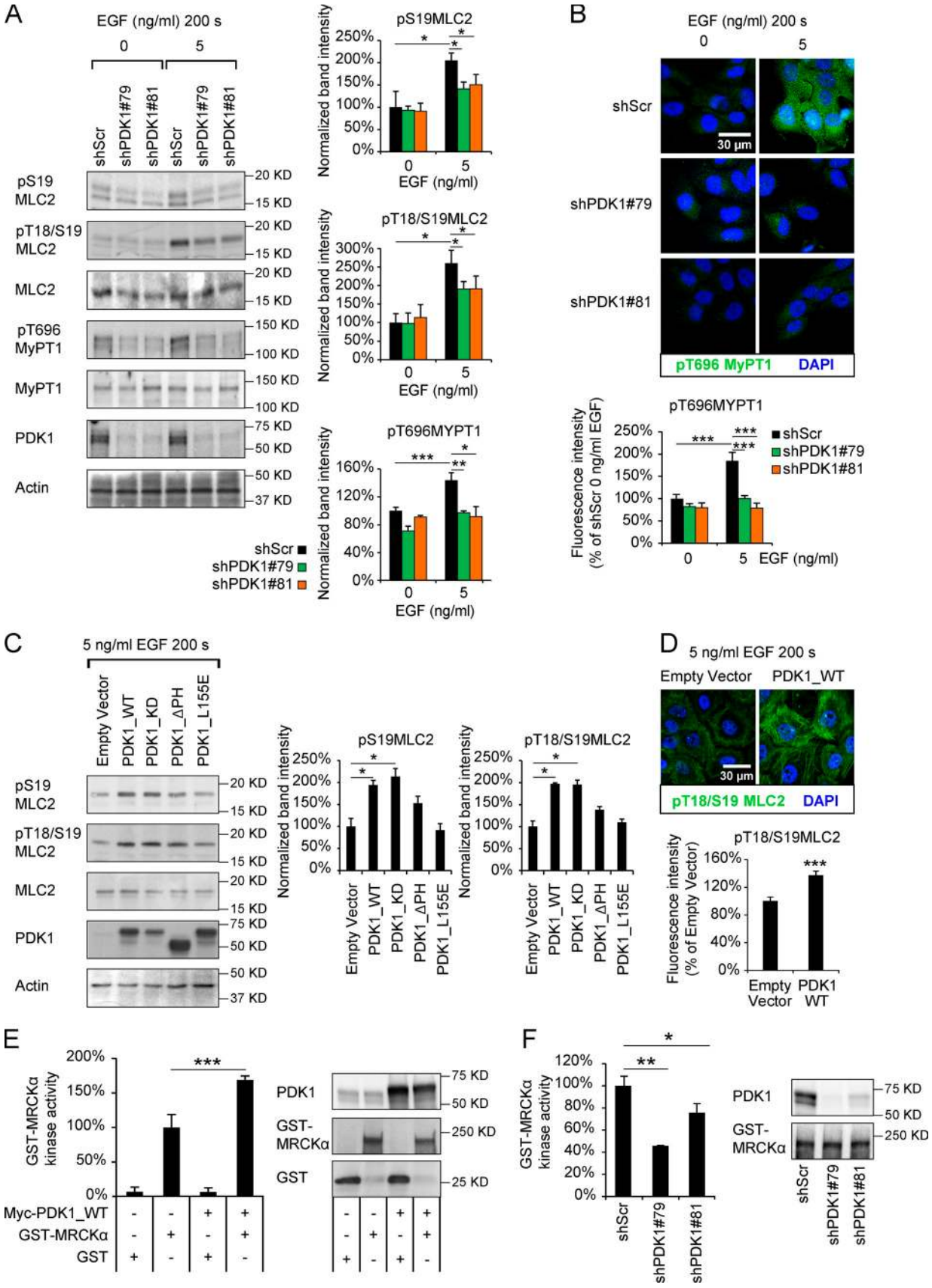

Figure 5. **PDK1 regulates MRCKα kinase activity.** (A) MCF10A, infected with lentiviral vectors coding for shScr, shPDK1 #79, or shPDK1 #81, were assayed for the phosphorylation of MLC2 on S19 or on T18/S19 and for the phosphorylation of MyPT1 on T696 in the absence or presence of 5 ng/ml EGF stimulation for 200 s. Band intensity quantification of pS19MLC2 pT18/S19MLC2 and pT696MYPT1 normalized to the total protein are represented as the

whether PDK1 was able to modulate the phosphorylation of MLC2 and MyPT1.

PDK1 knockdown reduced the EGF-induced increased phosphorylation of MCL2 on both S19 (Figs. 5 A and S3B) and T18/S19 (Figs. 5 A and S3 C). This reduction is even more evident on T696 of MyPT1 phosphorylation (Fig. 5, A and B). Moreover, the overexpression of PDK1_WT increased MLC2 phosphorylation at both single and double sites, and a similar effect was produced by PDK1_KD (Fig. 5, C and D). In contrast, the PDK1_L155E mutant was completely unable to increase MLC2 phosphorylation, whereas the PDK1_ΔPH mutant showed an intermediate effect (Fig. 5 C). To confirm that the regulation of MLC2 phosphorylation by PDK1 was dependent on MRCKα, we treated cells with the MRCK inhibitor chelerythrine chloride. No differences were observed between control and PDK1-overexpressing cells in the presence of MRCK inhibitor. Even in cells overexpressing both MRCKα and PDK1, the level of MLC2 phosphorylation was unchanged (Fig. S3 D). To further exclude the contribution of ROCK to PDK1-dependent regulation of MLC2, we treated cells with the ROCK inhibitor Y-27632. In these experimental conditions, MRCKα overexpression was able to induce an important increase of T18/S19 MLC2 phosphorylation, with further increases in cells overexpressing both PDK1_WT and MRCKα (Fig. S3 D).

Because PDK1 kinase activity was not required to increase MLC2 phosphorylation, we investigated whether the direct interaction between PDK1 and MRCKα could regulate the MRCKα activity. We performed in vitro kinase assays with recombinant purified proteins produced in eukaryotic cells. The catalytic region of MRCKα, described as constitutively active (Leung et al., 1998), displayed a high phosphorylation rate that did not change in the presence of GST-PDK1 (Fig. S3 E). The full-length form of MRCKα (GST-MRCKα), which instead is tightly regulated (Tan et al., 2001b), had low kinase activity and, unexpectedly, was not modulated by the addition of GST-PDK1_WT protein (Fig. S3 F). However, we obtained significant alterations of the kinase activity of GST-MRCKα when expressed in cells with different levels of PDK1. Specifically, the overexpression of PDK1_WT resulted in a significantly higher activity of MRCKα (Fig. 5 E), whereas the PDK1 silencing reduced the kinase activity of GST-MRCKα (Fig. 5 F). Collectively these results suggest that other molecular components are involved in the PDK1-dependent regulation of MRCKα.

PDK1 and MRCKα colocalize to the cell membrane upon EGF stimulation

We showed that PDK1 mutants that are unable to bind to PIP3 (PDK1_ΔPH and PDK1_K465E mutants) were defective in the regulation of directional migration (Fig. 2, B, D, and E). This suggested that PDK1 localization at the plasma membrane could be involved in this process. We analyzed by total internal reflection fluorescence (TIRF) microscopy the translocation at the plasma membrane of GFP-PDK1 and mCherry-MRCKα fusion proteins. EGF stimulation caused a rapid plasma membrane localization of GFP-PDK1_WT, reaching a maximum at 100 s after stimulation and slowly decreasing (Fig. 6 A and Video 3). Similarly, PDK1 mutants, GFP-PDK1_L155E, and GFP-PDK1_KD increased their plasma membrane localization upon EGF stimulation (Fig. 6 B and Video 4). As expected, GFP-PDK1_K465E was totally excluded from the plasma membrane (Fig. 6 B and Video 4). Stimulation with EGF also induced an increase of mCherry-MRCKα membrane localization (Fig. 6 C and Video 5). GFP-PDK1_WT and GFP-PDK1_KD cotranslocated with MRCKα to the plasma membrane with maximal colocalization at 200–300 s after EGF stimulation. Remarkably, the colocalized pixels were not randomly distributed but clustered in protrusive regions of adherent cell surface (Fig. 6, D and E; and Videos 6 and 7). Although we were not surprised that GFP-PDK1_K465E mutant, which is not able to bind PIP3, did not colocalize with MRCKα, more interesting was the lack of colocalization between GFP-PDK1_L155E and MRCKα (Fig. 6 E and Video 7). This indicates that both HM/PIF-binding pocket and plasma membrane anchorage are required to increase PDK1 and MRCKα colocalization in response to EGF.

PDK1 regulates MRCKα localization to lamellipodia

TIRF microscopy experiments suggested that PDK1 and MRCKα specifically colocalize at protrusive regions of the plasma membrane. We investigated whether these regions could be considered lamellipodia by transfecting cells with a plasmid coding for LifeAct-mTurquoise, which expressed a peptide that binds polymerized actin (F-actin), and by performing supplemental TIRF experiments. The colocalization of MRCKα/PDK1 upon EGF stimulation was much more evident in highly dynamic cellular protrusions with homogenous distribution of F-actin and rear-delimited by a more stable region characterized by condensed linear actin bundles (Fig. 7 A and Video 8). This description is coherent with the definition of lamellipodium and lamella, respectively (Ponti et al., 2004; Cai et al., 2008; Dang et al., 2013). The spatial proximity between PDK1 and MRCKα in lamellipodia was confirmed by in situ PLA and TIRF microscopy observation. The distribution of fluorescent spots showed a sharp accumulation in lamellipodia at 100 and 200 s upon EGF stimulation (Fig. 7 B). The overall number of fluorescent spots

mean ± standard error of the mean (error bars) of at least three independent experiments. (B) The same cells as in A were analyzed by immunofluorescence for MyPT1 phosphorylation: pT696MyPT1 antibody (green) and DAPI (blue). Total pixel intensity in cellular region of interest was quantified and expressed as normalization to shScr unstimulated cells. (C) MCF10A were infected with lentiviral vectors coding for PDK1_WT, PDK1_KD, PDK1_ΔPH, PDK1_L155E, or the empty vector and tested for the phosphorylation of MLC2 on S19 or on T18/S19. Band intensity quantification of pS19MLC2 and pT18/S19MLC2 normalized to the total protein are represented as the mean ± standard error of the mean (error bars) of three independent experiments. (D) The same cells as in C were analyzed by immunofluorescence for MLC2 phosphorylation: pT18/S19MLC2 antibody (green) and DAPI (blue) and quantification of pixel intensity. (E and F) GST-MRCKα or GST alone were pulled down and used for a kinase assay from HeLa cells infected with the following lentivirus: empty vector, PDK1_WT, shScr, shPDK1 #79, and shPDK1 #81. Each error bar represents the mean and standard error of the mean of five independent experiments. *, $P < 0.05$; **, $P < 0.01$; ***, $P < 0.001$.

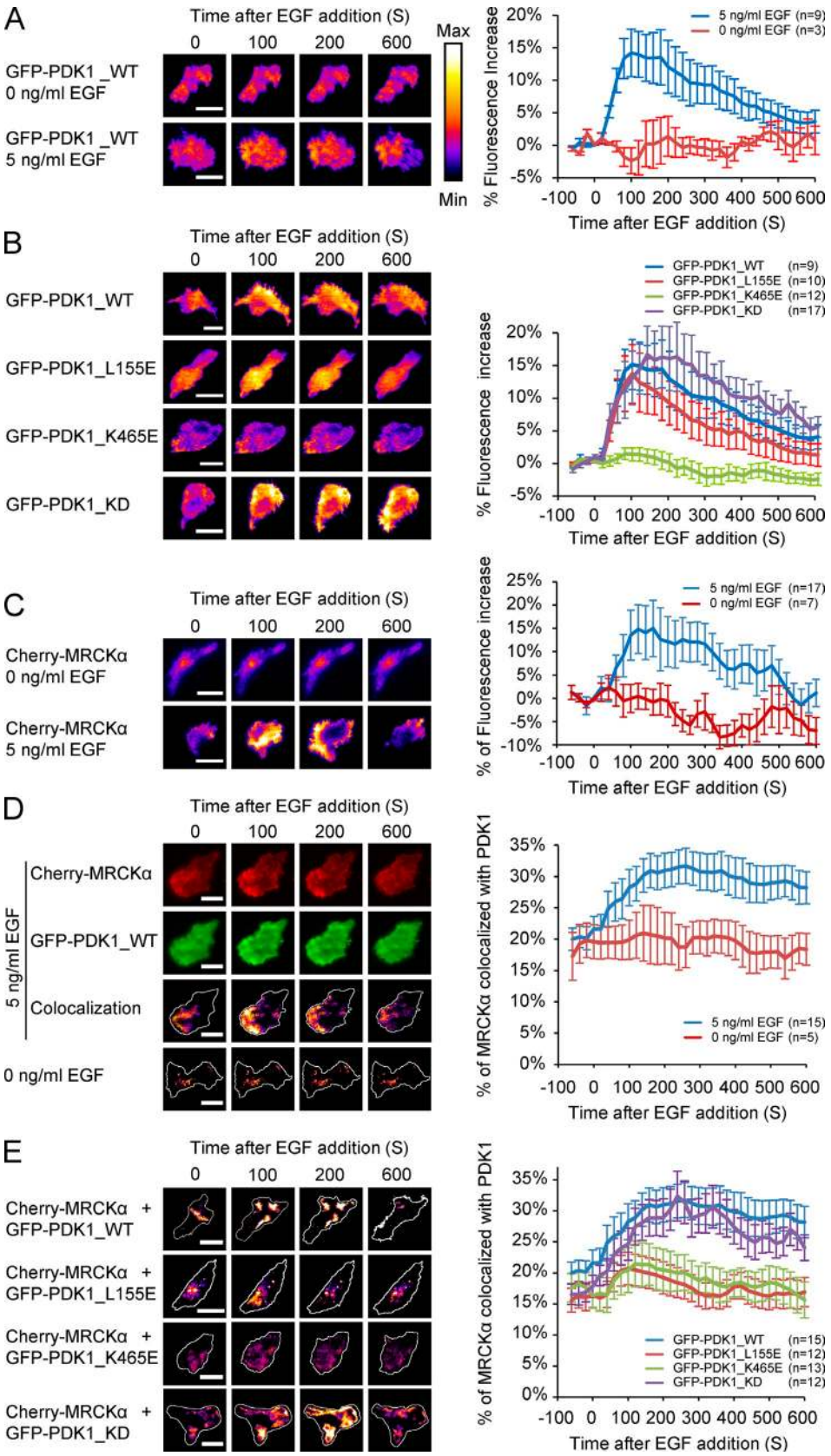

Figure 6. **PDK1 and MRCKα colocalize to the cell membrane upon EGF stimulation.** (A) MCF10A cells were transfected with GFP-PDK1_WT construct, then plasma membrane–bound PDK1 was detected through TIRF microscopy. Cells were stimulated with 5 ng/ml EGF or not stimulated, and imaged every 20 s. (A, left) TIRF fluorescence images of representative cells before and after EGF stimulation. (A, right) Time-dependent quantification of mean fluorescence intensity of the indicated number of experiments. Error bars represent the standard error of the mean. (B) MCF10A cells were transfected with GFP fused constructs of PDK1_WT, PDK1_L155E, PDK1_K465E, and PDK1_KD, then assayed as in A. (C) MCF10A cells expressing mCherry-MRCKα were assayed

per cell significantly increased upon EGF stimulation, reaching a maximum at around 200 s (Fig. S4 A).

Starting from these observations, we reasoned that PDK1 could regulate MRCKα localization to lamellipodia. To investigate this hypothesis, we evaluated by immunofluorescence the localization of MRCKα in cells either knocked down or overexpressing PDK1_WT and PDK1 mutants. The accumulation of MRCKα in lamellipodia by EGF stimulation (Fig. 8 A) was significantly reduced in PDK1-silenced cells (Fig. 8 B). In contrast, PDK1_WT overexpression determined an increase of cells showing high MRCKα localization to lamellipodia (Figs. 8 C and S4 B). A similar phenotype was observed in cells expressing PDK1_KD and PDK1_Δ50, whereas both PDK1_ΔPH and PDK1_L155E failed to allow the accumulation of MRCKα in lamellipodia (Fig. 8 C).

Lamellipodia retraction is regulated by PDK1 through MRCKα

The results showing that both PDK1 and MRCKα were enriched in lamellipodia, together with their role in directional migration, suggested that PDK1 could regulate lamellipodia dynamics through MRCKα. In response to EGF stimulation, MCF10A cells rapidly produced lamellipodia, which cause the extension of the cell surface to a maximum around 200–300 s from stimulation (Fig. 9 A). The extension of lamellipodia was then followed by lamellipodial retraction (Fig. 9 A). We precisely quantified these lamellipodia dynamics with a method based on the measurement of impedance as an indicator of cell surface extension. This method allows to clearly visualize both protrusion and retraction phases of lamellipodia on the whole cell population (see Materials and methods; Fig. 9 B).

PDK1 silencing significantly reduced both the protrusion and retraction phases (Fig. 9, C, D, and E). Furthermore, PDK1 overexpression increased both protrusion and retraction induced by EGF (Fig. 9, F, G, and H). Remarkably, MRCKα silencing specifically blocked the promoting effects of PDK1 overexpression in a retraction slope but not in a protrusion slope (Fig. 9, F and H). Collectively, these results indicate that PDK1 controls lamellipodia dynamics, but that only the retraction phase is completely dependent on PDK1-mediated regulation of MRCKα.

Collective cell invasion in a 3D model is induced by PDK1 overexpression

Cell migration plays a critical role in tumor cell dissemination and tissue invasion. Although most studies on this subject focus on two-dimensional setups, it is now well established that cell migration in three-dimensions displays distinctive features that cannot be found in 2D. To test whether PDK1 also drives cell migration and invasion in a 3D model of collective migration, we used MCF10DCIS.com cells, derived from MCF10A, which form DCIS-like lesions in in vivo mouse models, similar to primary human DCIS lesions, and spontaneously progress to invasive cancer.

Single MCF10DCIS.com cells seeded and embedded in 3D extracellular matrix gel grew as multicellular spheroids, which occasionally produced invasive protrusions (Fig. 10 A). Overexpression of PDK1_WT and PDK1_KD in MCF10DCIS.com cells resulted in a dramatic increase of the invasiveness when compared with control cells (Fig. 10, B and C). The overexpression of PDK1 affected the spheroidal structure and the actin basal localization observable in control spheroids. Moreover, PDK1 expression induced multicellular protrusions, typically composed by several cells, that maintained cell-to-cell contacts with actin cortical distribution (Fig. 10 D). We observed that the tip cells of these protrusions showed a particular actin enrichment at their leading edge (Fig. 10 D).

The quantification of the invasiveness of spheroids confirms the pro-invasive effect of both PDK1_WT and PDK1_KD overexpression (Fig. 10, E, F, and G). The PDK1 kinase–independent effect suggests a mechanism similar to that described in 2D migration. Thus, we verified whether MRCKα mediated the pro-invasive action of PDK1 by stably silencing MRCKα in MCF10DCIS.com overexpressing PDK1_WT or PDK1_KD (Fig. 10 E). The MRCKα knockdown reduced the invasive ability of spheroids overexpressing PDK1 to the level of control cells (Fig.10, F and G). In contrast, ROCK1 silencing (Fig. 10 H) did not significantly affect the number of invasive spheroids (Fig. 10 I) and invasive cells/spheroid (Fig. 10 J).

Altogether, these data suggest a specific role of PDK1 in 3D collective migration and invasion.

Discussion

Lamellipodia, together with filopodia, are the most frequently observed protrusive structures in cells migrating in a 2D environment (Ridley, 2011). Nevertheless it has been shown that lamellipodia are also present in 3D migration, together with protrusive structures that cannot be found in 2D, such as lobopodia or blebs (Petrie and Yamada, 2012; Petrie et al., 2012;). Here we describe a new regulative pathway involved in cell migration that links EGFR signaling to lamellipodia retraction through PDK1 and MRCKα.

We report that breast epithelial cells migrate toward an EGF gradient via a PI3K-dependent mechanism, in which PDK1 covers an essential role. Furthermore, PDK1 overexpression increases directional cell migration in nontransformed MCF10A cells and the invasive properties of preinvasive MCF10DCIS.com cells. This is consistent with data showing that PDK1 is amplified in some breast (Maurer et al., 2009) and prostate cancers (Choucair et al., 2012). Additionally, its overexpression correlates with more aggressive and invasive phenotypes (Maurer et al., 2009;

as in A. (D) MCF10A coexpressing GFP-PDK1_WT and mCherry-MRCKα were stimulated with 5 ng/ml EGF, and the colocalization channel was calculated as described in the Materials and methods section. In the colocalization channel, cell shapes are outlined in white. (E) EGF induced time-dependent variation of mCherry-MRCKα colocalization with GFP-PDK1_WT, GFP-PDK1_L155E, GFP-PDK1_K465E, or GFP-PDK1_KD. Error bars represent the standard error of the mean of *n* independent experiments. Bars, 20 µm.

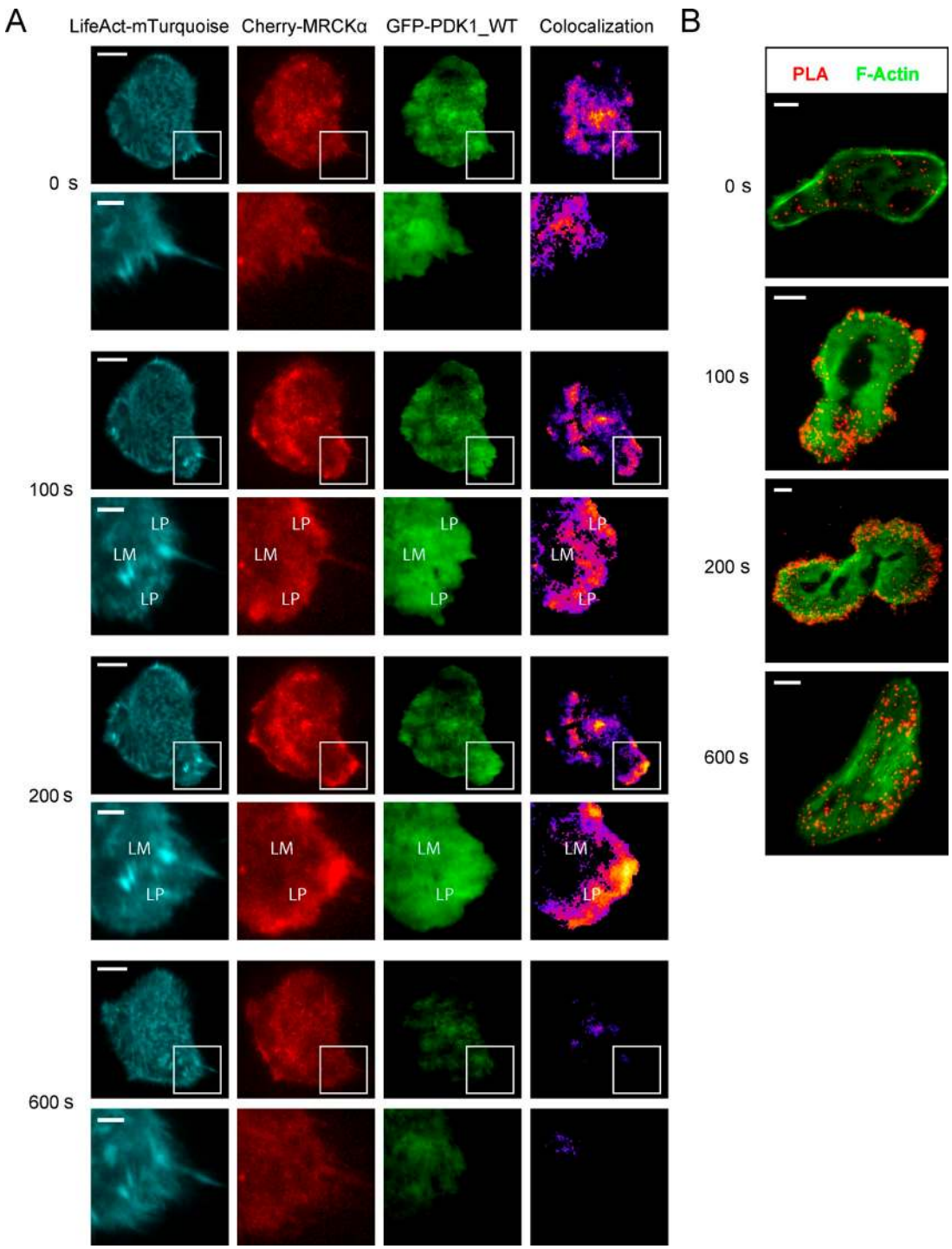

Figure 7. **PDK1 and MRCKα colocalize in nascent lamellipodia upon EGF stimulation.** (A) MCF10A cells, transfected with LifeAct-mTurquoise, mCherry-MRCKα, and GFP-PDK1_WT, were observed with TIRF microscopy set at 90 nm thickness, stimulated with 5 ng/ml EGF, and monitored every 20 s. Images show a representative cell before stimulation (0 s) and after stimulation (100 s, 200 s, and 600 s). The colocalization channel between mCherry-MRCKα and GFP-PDK1_WT was calculated as described in the Materials and methods section. Lamellipodia (LP) and lamella (LM) were identified on the basis of LifeAct-mTurquoise distribution. Enlargements (taken from the boxed regions above) were obtained by bicubic 4 × 4 interpolation of the original images. Bars: (top rows) 10 µm; (enlarged panels) 3 µm. (B) MCF10A cells were infected with a lentivirus coding for myc-PDK1 and, after EGF deprivation, stimulated with 5 ng/ml EGF. PLA of PDK1 and MRCKα was performed at different time points using, as detecting antibodies, anti–c-Myc produced in mouse and anti-MRCKα produced in rabbit. Fluorescent PLA spots close to the adherent surface were observed with TIRF microscopy set at 90 nm thickness. Cellular shape was identified by Phalloidin-488 staining. Bars, 10 µm.

Gagliardi et al., 2012; Scortegagna et al., 2013). Unexpectedly, we found that PDK1 exerts its pro-migratory activity in a kinase-independent manner. Indeed, PDK1 usually achieves its biological functions by phosphorylating substrates, such as Akt and RSK. However, it was reported that PDK1 activates, through kinase-independent mechanisms, Ral-GEF (Tian et al., 2002), PLCγ1 (Raimondi et al., 2012), and ROCK1 (Pinner and Sahai, 2008). Moreover, we found that PDK1-dependent

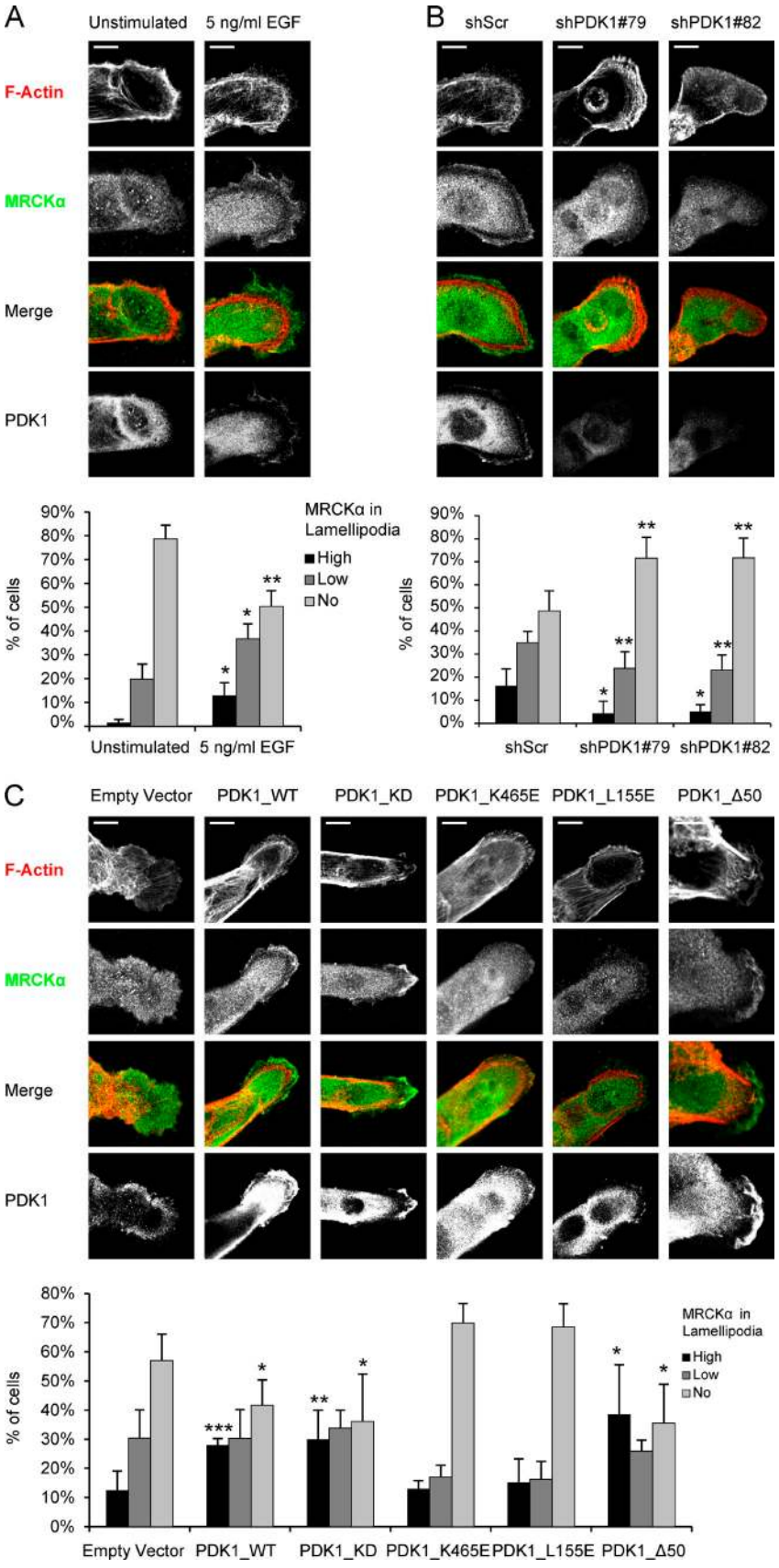

Figure 8. **PDK1 regulates MRCKα localization in lamellipodia.** (A–C) Evaluation of endogenous MRCKα localization in lamellipodia. In MCF10A cells, stained by immunofluorescence against MRCKα, lamellipodia (identified with F-actin) were divided in three classes on the level of MRCKα accumulation. MCF10A cells were tested for MRCKα accumulation in the presence or absence of EGF stimulation or, in the case of stable transduction, with: shScr, shPDK1 #79, shPDK1 #81, PDK1_WT, PDK1_KD, PDK1_ΔPH, PDK1_L155E, PDK1_Δ50, or empty lentiviral vectors. A number equal or superior to 100 cells was counted each condition. Each error bar represents the mean and standard error of the mean of three independent experiments. *, $P < 0.05$; **, $P < 0.01$; ***, $P < 0.001$. Bars, 10 μm.

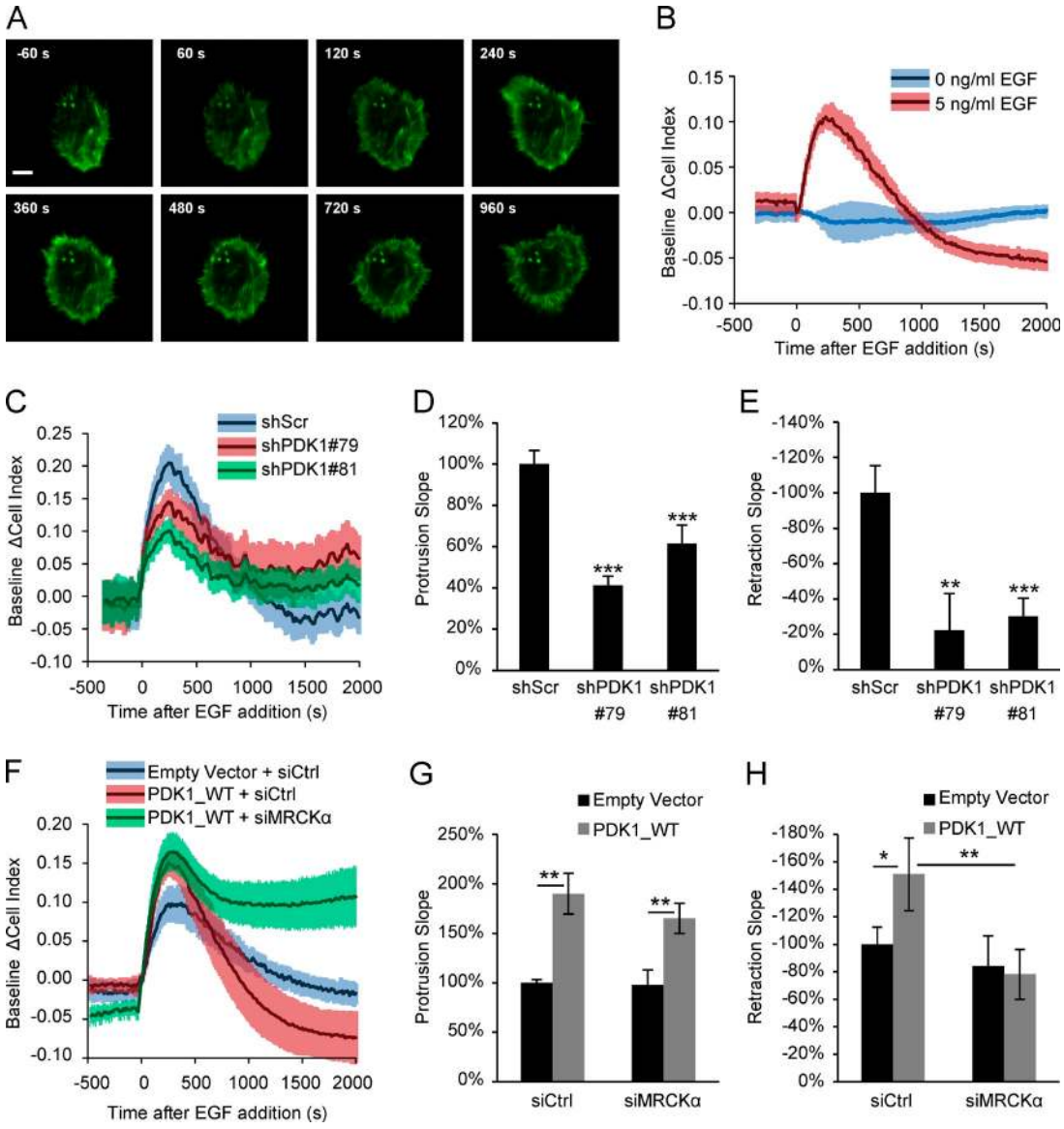

Figure 9. **PDK1 and MRCKα regulate lamellipodia retraction upon EGF stimulation.** (A) A representative MCF10A cell infected with a lentiviral vector coding for LifeAct-GFP, stimulated with EGF at t = 0 s, and imaged at different times before and after stimulation. Bar, 10 µm. (B) Time-lapse measurement of MCF10A electrical impedance in the presence or absence of EGF stimulation. Darker lines represent the mean values while lighter bands represent the area included between +SD and –SD. (C) Electrical impedance of MCF10A transduced with shScr, shPDK1 #79, or shPDK1 #81 upon EGF stimulation. (D and E) Protrusion and retraction slopes calculated from the electrical impedance. (F) Electrical impedance of MCF10A transduced with empty vector and PDK1_WT upon EGF stimulation. (G and H) Protrusion and retraction slopes calculated from the electrical impedance. Each error bar represents the mean and standard error of the mean of five independent experiments. *, P < 0.05; **, P < 0.01; ***, P < 0.001.

regulation of cell migration requires the integrity of the PDK1 PIF-binding pocket. For this reason, we focused our attention on Rho-GTPase–associated kinases, which have a highly conserved HM able to bind the PIF-binding pocket of PDK1, but lack a PDK1 phosphorylation site. All members of this family are myosin activators that directly phosphorylate MLC2 or the myosin phosphatase target subunit-1 MyPT1 (Pearce et al., 2010). The role of myosin contraction in migrating cells has traditionally been reported to be confined to tail retraction, but recent new data suggest a broader role, particularly in 3D cell migration (Petrie et al., 2012). Our data show that MCF10A migration toward the EGF gradient requires myosin activity, which is controlled by MRCK but not ROCK activity. Although ROCK is required for amoeboid-like cell migration, it has been suggested that MRCK is involved in mesenchymal cell migration (Wilkinson et al., 2005). Actually, MCF10A cells, which are nontransformed epithelial cells, retain the ability to migrate both as single cells, in a mesenchymal-like manner, and collectively, as an epithelial sheet. Therefore, it is conceivable that MRCK, instead of ROCK, regulates the MCF10A migration. In fact, MRCKα knockdown or inhibition hampers PDK1-induced directional cell migration, which suggests that MRCKα is locally activated in a PDK1-controlled manner. We also demonstrate that MRCKα associates with PDK1 through the interaction of the PDK1 PIF-binding pocket. Less clear is the role of MRCKβ, which associates with PDK1 but is not required for

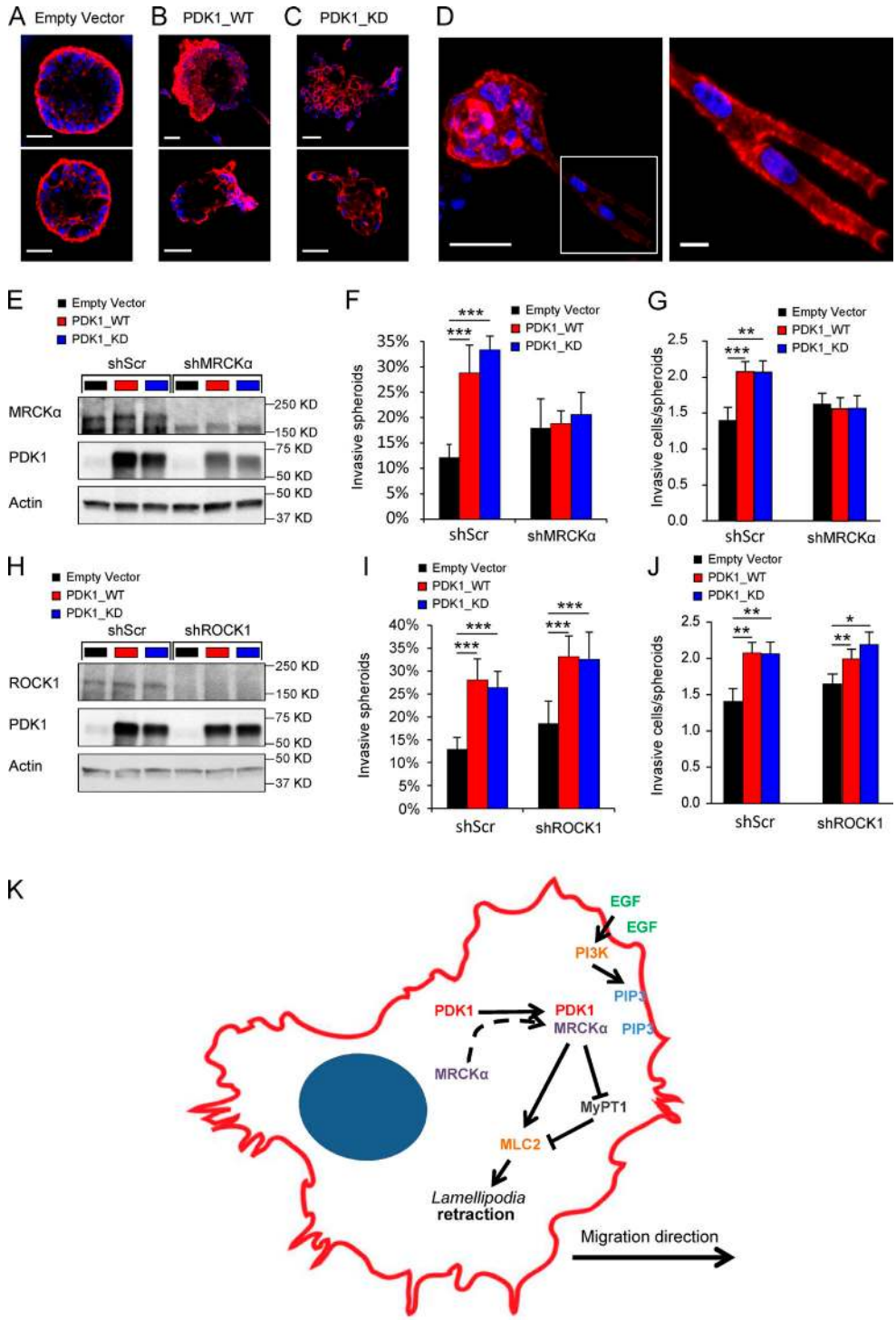

Figure 10. **PDK1 regulates 3D invasion through MRCKα in a kinase-independent manner.** (A–C) Representative spheroids of MCF10DCIS.com cells infected with empty vector (A) or vector overexpressing PDK1_WT (B) or PDK1_KD (C), and stained with Phalloidin (red) and DAPI (blue). Spheroids are shown as confocal equatorial sections. Bars, 50 μm. (D) Maximum projection of deconvolved confocal multistack of a PDK1_WT overexpressing spheroid and enlargement (taken from the boxed region). Bars: (left) 50 μm; (right) 10 μm. (E) Immunoblot showing expression levels of MRCKα and PDK1 in MCF10DCIS.com cells infected with empty vector and vectors overexpressing PDK1_WT or PDK1_KD and stably silenced with lentivirus coding for shRNA targeting MRCKα (shMRCKα) and compared with the shScr vector. (F) Percentage of invading spheroids per number of total spheroids. (G) Mean number of invasive cells per spheroid. (H) Immunoblot showing PDK1 and ROCK1 expression levels in MCF10DCIS.com infected with the empty vector or vectors overexpressing PDK1_WT or PDK1_KD, and stably silenced with lentivirus coding for shRNA targeting ROCK1 (shROCK1) and compared with the shScr vector. (I) Percentage of invading spheroids per number of total spheroids. (J) Mean number of invasive cells per spheroid. At least 200 spheroids were evaluated for each condition. Statistical significance was calculated based on four independent experiments with Fisher's exact test (F and I) and a Wilcoxon-Mann-Whitney test (G and J). *, $P < 0.05$; **, $P < 0.01$; ***, $P < 0.001$. (K) Graphical representation of the proposed model. EGF stimulation causes PI3K activation and PIP3 production at the plasma membrane. PDK1, which is localized in the cytoplasm in quiescent cells, rapidly translocates to the plasma membrane upon EGF stimulation and activates MRCKα in lamellipodia. This results in increased MyPT1 and MLC2 phosphorylation, determining myosin activity and lamellipodia retraction.

PDK1-induced migration. However, the silencing of MRCKβ up-regulates MRCKα expression, which may compensate for the loss of MRCKβ.

Experiments with spheroids of MCF10DCIS.com support the involvement of PDK1/MRCK signaling even during collective migration in a three-dimensional environment, which suggests a significant role for MRCK in the invasive process. Interestingly, it has been previously reported that collective invasion of the squamous cell carcinoma was dependent on MRCK signaling (Gaggioli et al., 2007).

Despite the direct interaction with MRCKα, PDK1 is not able to activate a purified MRCKα in vitro while it regulates MRCKα activity in intact cells or on crude cell lysates. This suggests an indirect mechanism of activation in which, for example, PDK1 could compete with a negative regulator of MRCKα. A similar model has been already proposed for ROCK1 (Pinner and Sahai, 2008). In any case, further efforts must be undertaken in order to understand such an unconventional type of regulation.

Conversely, results showing that PDK1, upon binding with PIP3, colocalizes with MRCKα, indicate that the interaction between PDK1 and MRCKα is increased by membrane translocation, similar to as previously described for PDK1 and Akt (Alessi et al., 1997). The regulation of MRCKα activity and the concomitant membrane localization constitute a precise spatio-temporal regulation orchestrated by PDK1 downstream of PI3K activation. This type of regulation is typically involved in processes that require a fine tuning of spatially and temporally localized intracellular signals, such as directional cell migration. In MCF10A cells, this regulation is particularly evident in lamellipodia retraction. We show that MRCKα does not regulate the formation phase of lamellipodia, but in contrast is involved in the lamellipodia retraction. However, PDK1 is able to regulate both lamellipodia protrusion and retraction, the latter being exerted through MRCKα. The localization of MRCKα in membrane protrusions has been previously reported, but its role in lamellipodia retraction and cell migration has not been fully explored (Tan et al., 2008).

Molecular mechanisms leading to lamellipodia formation or regulating cyclic protrusion of the leading edge have been described previously (Giannone et al., 2004; Bisi et al., 2013). PKA inhibition, for example, reduces the number of protrusions formed at the leading edge and increases their duration through a mechanism mediated by RhoA and RhoGDI (Tkachenko et al., 2011).

In contrast, the signaling pathways involved in lamellipodia retraction have received less attention, and the role of myosin in this process is particularly unclear. In the traditional model of cell motility, the generation of new actin filaments ensures lamellipodial growth, and protrusion continues until myosin II pulls the rear of the lamellipodial actin network, causing edge retraction and initiation of new adhesion sites (Ponti et al., 2004). In this model, it has been reported that MLCK, a kinase that phosphorylates myosin, is bound to the lamellipodial edge but that MLCK activation of myosin II is concentrated at the back of the lamellipodia, which suggests that periodic contractions release a fraction of MLCK that will be transported as periodic waves with actin filaments (Giannone et al., 2007). In contrast, a recently proposed model suggested that at the peak of protrusion myosin II filaments form in the lamellipodium, and a local network occurs that drives actin-arc formation and edge retraction (Burnette et al., 2011). In this model, MRCK localization to lamellipodium could locally activate myosin II and then could promote cell motility (Burnette et al., 2011). Whether PDK1/MRCK complex controls lamellipodia retraction through a mechanism like that of MLCK or if it activates myosin directly in the lamellipodium has yet to be investigated.

In summary, our work describes a new pathway regulating directional cell migration, which, through PI3K activity and PDK1 translocation to the membrane, activates MRCKα in cell protrusions resulting in lamellipodia retraction (Fig. 9 K). In addition, these findings call for a novel role for lamellipodia retraction linked to directional cell migration.

Materials and methods

Cell lines

MCF10A (CRL-10317), 293T (CRL-11268), and HeLa (CCL-2) cell lines were obtained from the ATCC resource center. MCF10DCIS.com (Miller et al., 2000) were kindly provided by the G. Scita laboratory (IFOM, Milan, Italy). All experiments were performed on cell lines that had been passaged for <3 mo after thawing. 293T and HeLa cells were cultured in DMEM (catalogue no. D5546; Sigma-Aldrich). The culture medium was supplemented with 10% FBS (catalogue no. 10270; Gibco), 200 U/ml of penicillin, and 200 µg/ml streptomycin (catalogue no. 67513; Sigma-Aldrich). MCF10A and MCF10DCIS.com cells were cultured as described previously (Debnath et al., 2003). SiRNAs were transfected in MCF10A cells using Oligofectamin (Life Technologies). Pools of siRNA targeting MRCKα (L-003814-00), MRCKβ (L-004075-00), ROCK1 (M-003536-02), and control nontargeting siRNA #1 (D-001810-01-05) were purchased from GE Healthcare.

Antibodies and reagents

Rabbit anti-Akt1 (2H10), rabbit anti-pT308Akt (244F9), rabbit anti-pS241PDK1, rabbit anti-PDK1, rabbit anti-pS19MLC2, rabbit anti-pT18/S19 MLC2, and rabbit anti-MLC2 were purchased from Cell Signaling Technology. Rabbit anti-MRCKα (H-90), goat anti-actin (C-11), mouse anti-GST (B-14), goat anti-ROCK1 (K-18), mouse anti–c-Myc (SC-40), and mouse anti-PDK1 (E-3) were from Santa Cruz Biotechnology, Inc. Mouse anti-FLAG and mouse anti-CDC42BPB clone 2F4 (anti-MRCKβ) were from Sigma-Aldrich. Rabbit anti-pT696MyPT1 was from EMD Millipore. Rabbit anti-MyPT1 was from EMD Millipore. Rabbit anti-GFP was from Life Technologies. Human EGF was purchased from R&D Systems. Human HGF was from PeproTech. LY294002 was from Cell Signaling Technology. Y-27632 was from EMD Millipore. Chelerythrine chloride was from Sigma-Aldrich. GSK2334470 was provided by the MRC Protein Phosphorylation Unit. Alexa Fluor 647, 555, and 488 Phalloidin were obtained from Invitrogen.

Plasmid constructs

Myc-tagged PDK1, PDK1-KD (K111N), PDK1-ΔPH, PDK1-L155E, and PDK1-Δ50, previously cloned into PINCO retroviral vector (Primo et al., 2007), were subcloned into a third-generation lentiviral vector pCCL.sin.cPPT.polyA.CTE.eGFP.minhCMV.hPGK.Wpre (Follenzi et al., 2000; Amendola et al., 2005) as described previously (Gagliardi et al., 2012). K465E point mutation was introduced using the following primers: FW (5′-GGCCCAGTGGATGAGCGGAAGGGTTTATTT), and RE (AAATAAACCCTTCCGCTCATCCACTGGGCC-3′).

PDK1_WT, PDK1-KD (K111N), PDK1-L155E, and PDK1_K465E mutants were cloned in pDONR/zeo using Gateway BP Clonase (Invitrogen). To perform the BP recombination, we performed a PCR reaction using the following primers: attB1-PDK1 (5′-ACAAGTTTGTACAAAAAAGCAGGCTTAACCATGGCCAGGACCACCAGCCAGCTGTATGAC-3′), attB1-PDK1Δ50 (5′-ACAAGTTTGTACAAAAAAGCAGGCTTAACCATGGACGGCACTGCAGCCGAGCCTC-3′), attB2-PDK1 (5′-ACCACTTTGTACAAGAAAGCTGGGTTGCCCTGCACAGCGGCGTCCGGGTGG-3′), and attB2-PDK1ΔPH (5′-ACCACTTTGTACAAGAAAGCTGGGTTGCCCTGGTGCCAAGGGTTTCCGCCAGCCTG-3′).

MRCKα WT and MRCKαCAT_WT were provided by the T. Leung laboratory (Institute of Molecular and Cell Biology, A-STAR, Singapore; Leung et al., 1998; Tan et al., 2001b) and cloned into pDONR/zeo using Gateway

BP Clonase (Invitrogen). We used the following primers: attB1-MRCKα (5′-ACAAGTTTGTACAAAAAAGCAGGCTTAACCATGTCTGGAGAAGTGCGTTTGAGGCAGTTGGAGCAG-3′), attB2-MRCKα (5′-ACCACTTTGTACAAGAAAGCTGGGTTGCCCGGGTCCCAGCTCCCGCGGTC-3′), and attB2-MRCKαCAT (5′-ACCACTTTGTACAAGAAAGCTGGGTTGCCCTGCAGAGCTTGGACAGTCTGTGTTGACTCTTG-3′).

The sequence of catalytic domain of MRCKβ, Addgene plasmid 50759 (Ando et al., 2013), was cloned into pDONR/zeo using the following primers: attB1-MRCKβ (5′-ACAAGTTTGTACAAAAAAGCAGGCTTAACCATGTCGGCCAAGGTGCGGCTCAAGAAGCTGGAGC-3′) and attB2-MRCKβCAT (5′-ACCACTTTGTACAAGAAAGCTGGGTTGCCGTGGAGGGACTGCACGGTCTGGGTGGAC-3′).

The constructs previously cloned into pDONR/zeo were transferred through Gateway LR Clonase in the following destination vectors: pcDNA-DEST47 (C-Term GFP), in pcDNA-DEST53 (N-Term GFP), in pcDNA-C-mCherry (C-term mCherry), and in pDEST27 (GST-N-Term Tag; all from Invitrogen).

Lentivirus production

Lentivirus vectors were produced as described previously (Gagliardi et al., 2012). In brief, for PDK1 stable silencing, two pLKO.1 lentiviral vectors carrying PDK1 targeting shRNA called, respectively, shPDK1 #79 (TRCN0000039779; Sigma-Aldrich) and shPDK1#81 (TRCN0000039781) were used. For MRCKα and ROCK1 stable silencing, we used the following constructs: TRCN0000001332, TRCN0000001333, TRCN0000195202, and TRCN0000121312. A vector leading the expression of a scrambled not targeting shRNA, called shScr, Addgene plasmid 1864 (Sarbassov et al., 2005), was used as a negative control. pCCL.sin.cPPT.polyA.CTE.eGFP.minhCMV.hPGK.Wpre lentiviral vector (Follenzi et al., 2000; Amendola et al., 2005) was used for PDK1 constructs expression. This vector led the expression, through a bidirectional hPGK promoter, of both PDK1 constructs and GFP. A plasmid expressing only GFP was used as a negative control (empty vector). All viruses were produced as described in The RNA Consortium's shRNA guidelines. Cell infection was performed with an MOI equal to 1 for pLKO.1 and an MOI equal to 5 for pCCL.sin.cPPT.polyA.CTE.eGFP.minhCMV.hPGK.Wpre lentiviral vectors, in the presence of 8 µg/ml Polybrene (H-9268; Sigma-Aldrich).

Chemotaxis and wound healing assay

1 d before the assay, MCF10A cells were split in order to reach a confluence <30% at the time of the assay. MCF10A were detached from culture plates using a Trypsin-EDTA solution (Sigma-Aldrich), then resuspended in DMEM at 2.5×10^5 density. 400 µl of cell suspension (containing 10^5 cells) were seeded into 8.0-µm pore size inserts (BD). Cells were left to migrate toward 750 µl of DMEM containing various concentrations of EGF or HGF and compared with DMEM alone, as a negative control. Then cells were maintained in a humidified incubator at 37°C plus 5% CO_2 for 6 h (EGF) or 24 h (HGF). Nonmigrated cells were removed with a cotton tip. The inserts were fixed in PBS and 2.5% glutaraldehyde for 20 min and stained with Crystal Violet dissolved in H_2O 20% Methanol. Two fields for each insert were imaged with a 5× objective lens. Cells were counted by image thresholding with ImageJ.

Wound healing scratch assay was performed as described previously (Primo et al., 2010). In brief, 2×10^6 GFP-tagged MCF10A were seeded on 24-well plates the day before the assay. Cells were wounded by dragging a plastic pipette tip across the cell layer. Alternatively, GFP-tagged MCF10A were seeded at low density (10^4 cells) on 24-well plates to ensure a single cell distribution. Cell movement was followed by inverted-phase contrast and fluorescent time-lapse microscopy (Microsystems LAS AF 6500/7000 [Leica] equipped with an HC PL FLUOTAR 10×/0.30 PH objective lens) every 20 min. Time-lapse image sequences of wound healing or sparse cell motility were analyzed and cell tracked with MetaMorph 7.0 (Molecular Devices). The persistence was calculated as the distance between the start and the end point divided by the path length of a cell trajectory, whereas the FMI was calculated as the orthogonal projection in the direction of migration of the distance between the start and the end point divided by the path length of a cell trajectory.

Viability assay

Viability was evaluated with an MTT assay. Cells were cultured for 24 h in 6-well plates, then 0.2 mg/ml of MTT in culture medium without Phenol red was added. After 3 h of incubation with MTT, the supernatant was removed, and 200 µl of DMSO was added to dissolve the formazan crystal. The optical density value of each sample was measured at a wavelength of 595 nm.

Immunoprecipitation and immunoblotting

HeLa cells stable transduced with empty vector, PDK1_WT, and PDK1_L155E lentivirus were transfected with pXJ40-FLAG-MRCKα (Leung et al., 1998; Tan et al., 2001b). Cell proteins were extracted with lysis buffer (50 mM Tris-HCl, 150 mM NaCl, 1 mM PMSF, 100 µM $ZnCl_2$, 1% Triton X-100, 1 mM Na_3VO_4, 10 mM NaF, and 1:1,000 protease inhibitor cocktail; Sigma-Aldrich). Cell lysates were incubated with anti-Flag antibody (Sigma-Aldrich) or negative control mouse IgG for 2 h; immune complexes were recovered on anti–mouse IgG-Agarose (Sigma-Aldrich). Proteins were separated by SDS-PAGE electrophoresis, transferred to polyvinylidene difluoride (PVDF) membrane (Bio-Rad Laboratories), incubated with primary antibody, and visualized by ECL.

Pull-down and kinase assay

pDEST27-MRCKα_CAT or pDEST27-MRCKβ_CAT plasmids were transfected in 293T cells with calcium phosphate (Promega). After 36 h, cell lysates were extracted using lysis buffer. GST-tagged protein was isolated through Glutathione Sepharose 4B beads (GE Healthcare). Meanwhile, lysates from MCF10A cells stably infected with the empty vector, PDK1_WT, PDK1_L155E, or PDK1_K465E were extracted using the same lysis buffer. The GST-tagged proteins isolated from 293T bound to glutathione beads were used to pull down proteins from MCF10A extracts. The pulled-down proteins were dissociated using reducing Laemmli buffer (62.5 mM Tris-HCl, pH 6.8, 2% SDS, and 10% glycerol) and analyzed by immunoblotting.

MRCKα kinase assay was performed by transfecting pDEST27-GST-MRCKα in 293T or HeLa cells overexpressing or silenced for PDK1. After 36 h, cell lysates were extracted using the kinase buffer (25 mM Hepes, 300 mM NaCl, 1 mM PMSF, 1.5 mM $MgCl_2$, 0.5% Triton X-100, 20 mM Na-β glycerophosphate, 1 mM Na_3VO_4, 0.2 mM EDTA, and 1:1,000 protease inhibitor cocktail; Sigma-Aldrich). Purified GST-MRCKα was assayed for its ability to phosphorylate T696 of recombinant MyPT1 (CSA001; Millipore).

PLA

PLA was performed according to the Olink Bioscience's protocol using Duolink II reagents with minor changes. After blocking and primary antibody staining, PLA anti–mouse MINUS and anti–rabbit PLUS probes were diluted 1:5 in PBS 1% donkey serum and incubated for 1 h at 37°C in a preheated humidity chamber. Subsequent ligation and amplification steps were performed using Duolink II Detection kit according to the manufacturer's instructions.

Live TIRF microscopy

GFP-PDK1_WT, GFP-PDK1_KD, GFP-PDK1_L155E, GFP-PDK1_K465E, mCherry-MRCKα, LifeAct-EGFP (Riedl et al., 2008), and LifeAct-mTurquoise (Addgene Plasmid 36201; Goedhart et al., 2012) were transfected in MCF10A cells using X-tremeGENE Transfection Reagents (Roche). Then cells were seeded at low density on glass bottom plates (MatTek Corporation) coated with 1 µg/ml fibronectin (Sigma-Aldrich). After starvation overnight in medium without growth factors (DMEM supplemented 200 U/ml of penicillin and 200 µg/ml streptomycin), cells were placed on an inverted microscope equipped with a 37°C humidified chamber with 5% CO_2, and visualized using a fluorescence microscope (True MultiColor Laser TIRF Leica AM TIRF MC; Leica) equipped with a 63× oil immersion objective lens (HCX Plan-Apochromat 63×/1.47 oil CORR TIRF) and an EM-CCD camera (C9100-02; Hamamatsu Photonics). Images were acquired with LAS AF6000 modular system software (Leica). We quantified fluorescence intensity in regions of interest in multiple channels with ImageJ software. Colocalization analysis was performed with the Imaris 6.3 (Bitplane) software colocalization module by determining thresholds in a systematic way. In the image histogram of the prestimulus fluorescence channels, we identified two distinct peaks: one for the background and one for the fluorescence intensity within the cell. The mode of the second peak for each channel was used as the threshold for the whole sequence of images. Once the images were thresholded, we considered the pixels that were in the intersection of the two thresholded images (in each time frame) to be colocalized pixels. For each time frame, we then calculated the sum of the intensity of the MRCKα channel in the intersected pixels divided by the total MRCKα intensity within the thresholded image and multiplied it by 100.

Immunofluorescence and confocal microscopy

MCF10A cells cultured on chamber slides were fixed in freezing cold methanol or in 3.7% paraformaldehyde, permeabilized for 10 min in PBS 0.1% Triton X-100 (T8294; Sigma-Aldrich), washed three times with PBS, and saturated in 10% donkey serum (Sigma-Aldrich). The primary antibodies were left on the slices overnight in PBS plus 10% donkey serum at a 1:100 dilution at 4°C. The secondary staining was performed at 25°C for 1 h with fluorescent dye–conjugated antibodies (Alexa Fluor 488, Alexa Fluor 555, and Alexa Fluor 405; Invitrogen). Images were acquired at room temperature with a confocal laser-scanning microscope (SPEII DM5500 CSQ; Leica)

equipped with a 63×/1.30 HCX Plan-Apochromat oil-immersion objective lens (ACS APO 63×/1.30 oil CS 0.17/E, 0.16) using Leica LAS AF software. Images were analyzed with ImageJ software.

Electrical impedance measurement of lamellipodia dynamics

Lamellipodia formation was measured by the Xcelligence system (Acea Biosciences, Inc.). 3×10^3 MCF10A cells were seeded into each well of E-plate 16. After 24 h of adhesion, cells were starved overnight in 100 µl of serum-free DMEM. The impedance was measured with an RTCA DP Analyzer (Acea Biosciences, Inc.) every 7 s for 5 min after the beginning of the measurement. 100 µl of 5 ng/ml EGF was added to each well, and cells were monitored for about an hour. The baseline Δ cell index was calculated using as Δ time the time of EGF addition and as a baseline the unstimulated cells curve. The protrusion slope was calculated on the first 100 s from EGF stimulus, whereas the retraction slope was calculated from the peak of the curve to 600 s after the peak itself. To visualize time-dependent lamellipodia extension and retraction at TIRF microscopy, we infected MCF10A with a virus expressing LifeAct-EGFP.

MCF10DCIS.com spheroids

3D culture of MCF10DCIS.com spheroids was performed by seeding isolated MCF10DCIS.com cells (10^3) embedded in 50 µl of Matrigel. Medium was refreshed every 2–3 d. After 8 d, spheroids were fixed in 3.7% paraformaldehyde, permeabilized for 10 min in PBS with 0.5% Triton X-100 (T8294; Sigma-Aldrich) and stained with Phalloidin-555 and DAPI. Spheroid images were acquired at room temperature with a confocal laser-scanning microscope (SPEII DM5500 CSQ; Leica) equipped with a 20× oil-immersion objective lens (ACS APO 20×/0.60 Imm CS) using Leica LAS AF software. Images were analyzed by ImageJ software. The percentage of invasive spheroids and the extent of invasion were obtained by manually counting the presence and the number of cells invading the extracellular matrix from the spheroid, identifying invading cells by both DAPI and Phalloidin staining.

Statistical analysis

For box plot representations, the central line depicts median values; the upper and the lower hinges represent the 75th and 25th percentiles, respectively; and the upper and the lower whiskers represent the 90th and 10th percentiles, respectively. All the remaining data are represented as mean value of both technical and biological replicates, whereas error bars give the standard error of the mean. Statistical analysis was performed using GraphPad Prism software (GraphPad Software). Statistical significance was determined by a Student's *t* test or one-way analysis of variance, with $P < 0.05$ considered significant.

Online supplemental materials

Fig. S1 shows additional experiments and controls confirming that PDK1 specifically regulates directional cell migration toward EGF. Fig. S2 shows additional experiments supporting the kinase-independent role of PDK1 in directional cell migration toward EGF and HGF. Fig. S3 shows PDK1 pull-down with GST-MRCKβ_CAT and additional experiments on PDK1 regulation of MRCKα activity. Fig. S4 shows the quantification of the PLA signal with TIRF microscopy and an immunofluorescence of MRCKα in PDK1-overexpressing cells compared with control cells. Tables S1 and S2 show the Blast search for proteins having highly conserved HM consensus sequences. Videos 1 and 2 show time-lapse movies of wound healing assays made with cells silenced for or overexpressing PDK1, respectively. Videos 3, 4, 5, 6, and 7 are the time-lapse movies relative to the images shown in Fig. 6. Video 8 is the time-lapse movie relative to the images shown in Fig. 7. Online supplemental material is available at http://www.jcb.org/cgi/content/full/jcb.201312090/DC1.

We thank Dr. Giorgio Scita for suggestions and critical reading of the manuscript.

This work was supported by Associazione Italiana per la Ricerca sul Cancro (AIRC) investigator grants IG (10133 to F. Bussolino, and 9158 to L. Primo); AIRC 5x1000 (12182 to F. Bussolino), Fondazione Piemontese per la Ricerca sul Cancro-ONLUS (Intramural Grant 2010 to L. Primo), Fondo Investimenti per la Ricerca di Base RBAP11BYNP (Newton to F. Bussolino and L. Primo), University of Torino Compagnia di San Paolo (RETHE to F. Bussolino, GeneRNet to L. Primo), FP7-ICT-2011-8 Biloba (contract 318035), and Consiglio Nazionale delle Ricerche (CNR; grant "Personalized Medicine" to F. Bussolino). P.A. Gagliardi is supported by a triennial FIRC fellowship (15026).

The authors declare no competing financial interests.

Submitted: 19 December 2013
Accepted: 24 June 2014

References

Alessi, D.R., S.R. James, C.P. Downes, A.B. Holmes, P.R. Gaffney, C.B. Reese, and P. Cohen. 1997. Characterization of a 3-phosphoinositide-dependent protein kinase which phosphorylates and activates protein kinase Bα. *Curr. Biol.* 7:261–269. http://dx.doi.org/10.1016/S0960-9822(06)00122-9

Amano, M., M. Ito, K. Kimura, Y. Fukata, K. Chihara, T. Nakano, Y. Matsuura, and K. Kaibuchi. 1996. Phosphorylation and activation of myosin by Rho-associated kinase (Rho-kinase). *J. Biol. Chem.* 271:20246–20249. http://dx.doi.org/10.1074/jbc.271.34.20246

Amano, M., K. Chihara, N. Nakamura, T. Kaneko, Y. Matsuura, and K. Kaibuchi. 1999. The COOH terminus of Rho-kinase negatively regulates rho-kinase activity. *J. Biol. Chem.* 274:32418–32424. http://dx.doi.org/10.1074/jbc.274.45.32418

Amendola, M., M.A. Venneri, A. Biffi, E. Vigna, and L. Naldini. 2005. Coordinate dual-gene transgenesis by lentiviral vectors carrying synthetic bidirectional promoters. *Nat. Biotechnol.* 23:108–116. http://dx.doi.org/10.1038/nbt1049

Ando, K., S. Fukuhara, T. Moriya, Y. Obara, N. Nakahata, and N. Mochizuki. 2013. Rap1 potentiates endothelial cell junctions by spatially controlling myosin II activity and actin organization. *J. Cell Biol.* 202:901–916. http://dx.doi.org/10.1083/jcb.201301115

Biondi, R.M., A. Kieloch, R.A. Currie, M. Deak, and D.R. Alessi. 2001. The PIF-binding pocket in PDK1 is essential for activation of S6K and SGK, but not PKB. *EMBO J.* 20:4380–4390. http://dx.doi.org/10.1093/emboj/20.16.4380

Bisi, S., A. Disanza, C. Malinverno, E. Frittoli, A. Palamidessi, and G. Scita. 2013. Membrane and actin dynamics interplay at lamellipodia leading edge. *Curr. Opin. Cell Biol.* 25:565–573. http://dx.doi.org/10.1016/j.ceb.2013.04.001

Blay, J., and K.D. Brown. 1985. Epidermal growth factor promotes the chemotactic migration of cultured rat intestinal epithelial cells. *J. Cell. Physiol.* 124:107–112. http://dx.doi.org/10.1002/jcp.1041240117

Burnette, D.T., S. Manley, P. Sengupta, R. Sougrat, M.W. Davidson, B. Kachar, and J. Lippincott-Schwartz. 2011. A role for actin arcs in the leading-edge advance of migrating cells. *Nat. Cell Biol.* 13:371–382. http://dx.doi.org/10.1038/ncb2205

Cai, L., A.M. Makhov, D.A. Schafer, and J.E. Bear. 2008. Coronin 1B antagonizes cortactin and remodels Arp2/3-containing actin branches in lamellipodia. *Cell*. 134:828–842. http://dx.doi.org/10.1016/j.cell.2008.06.054

Choucair, K.A., K.P. Guérard, J. Ejdelman, S. Chevalier, M. Yoshimoto, E. Scarlata, L. Fazli, K. Sircar, J.A. Squire, F. Brimo, et al. 2012. The 16p13.3 (PDPK1) genomic gain in prostate cancer: a potential role in disease progression. *Transl. Oncol*. 5:453–460. http://dx.doi.org/10.1593/tlo.12286

Currie, R.A., K.S. Walker, A. Gray, M. Deak, A. Casamayor, C.P. Downes, P. Cohen, D.R. Alessi, and J. Lucocq. 1999. Role of phosphatidylinositol 3,4,5-trisphosphate in regulating the activity and localization of 3-phosphoinositide-dependent protein kinase-1. *Biochem. J.* 337:575–583. http://dx.doi.org/10.1042/0264-6021:3370575

Dang, I., R. Gorelik, C. Sousa-Blin, E. Derivery, C. Guérin, J. Linkner, M. Nemethova, J.G. Dumortier, F.A. Giger, T.A. Chipysheva, et al. 2013. Inhibitory signalling to the Arp2/3 complex steers cell migration. *Nature*. 503:281–284. http://dx.doi.org/10.1038/nature12611

Debnath, J., S.K. Muthuswamy, and J.S. Brugge. 2003. Morphogenesis and oncogenesis of MCF-10A mammary epithelial acini grown in three-dimensional basement membrane cultures. *Methods*. 30:256–268. http://dx.doi.org/10.1016/S1046-2023(03)00032-X

Di Cunto, F., E. Calautti, J. Hsiao, L. Ong, G. Topley, E. Turco, and G.P. Dotto. 1998. Citron rho-interacting kinase, a novel tissue-specific ser/thr kinase encompassing the Rho-Rac-binding protein Citron. *J. Biol. Chem.* 273:29706–29711. http://dx.doi.org/10.1074/jbc.273.45.29706

Follenzi, A., L.E. Ailles, S. Bakovic, M. Geuna, and L. Naldini. 2000. Gene transfer by lentiviral vectors is limited by nuclear translocation and rescued by HIV-1 pol sequences. *Nat. Genet.* 25:217–222. http://dx.doi.org/10.1038/76095

Gaggioli, C., S. Hooper, C. Hidalgo-Carcedo, R. Grosse, J.F. Marshall, K. Harrington, and E. Sahai. 2007. Fibroblast-led collective invasion of carcinoma cells with differing roles for RhoGTPases in leading and following cells. *Nat. Cell Biol.* 9:1392–1400. http://dx.doi.org/10.1038/ncb1658

Gagliardi, P.A., L. di Blasio, F. Orso, G. Seano, R. Sessa, D. Taverna, F. Bussolino, and L. Primo. 2012. 3-phosphoinositide-dependent kinase 1 controls breast tumor growth in a kinase-dependent but Akt-independent manner. *Neoplasia*. 14:719–731.

Giannone, G., B.J. Dubin-Thaler, H.G. Döbereiner, N. Kieffer, A.R. Bresnick, and M.P. Sheetz. 2004. Periodic lamellipodial contractions correlate with rearward actin waves. *Cell*. 116:431–443. http://dx.doi.org/10.1016/S0092-8674(04)00058-3

Giannone, G., B.J. Dubin-Thaler, O. Rossier, Y. Cai, O. Chaga, G. Jiang, W. Beaver, H.G. Döbereiner, Y. Freund, G. Borisy, and M.P. Sheetz. 2007. Lamellipodial actin mechanically links myosin activity with adhesion-site formation. *Cell*. 128:561–575. http://dx.doi.org/10.1016/j.cell.2006.12.039

Goedhart, J., D. von Stetten, M. Noirclerc-Savoye, M. Lelimousin, L. Joosen, M.A. Hink, L. van Weeren, T.W. Gadella Jr., and A. Royant. 2012. Structure-guided evolution of cyan fluorescent proteins towards a quantum yield of 93%. *Nat. Commun.* 3:751. http://dx.doi.org/10.1038/ncomms1738

Ikebe, M., and D.J. Hartshorne. 1985. Phosphorylation of smooth muscle myosin at two distinct sites by myosin light chain kinase. *J. Biol. Chem.* 260:10027–10031.

Kaliman, P., and E. Llagostera. 2008. Myotonic dystrophy protein kinase (DMPK) and its role in the pathogenesis of myotonic dystrophy 1. *Cell. Signal.* 20:1935–1941. http://dx.doi.org/10.1016/j.cellsig.2008.05.005

Kimura, K., M. Ito, M. Amano, K. Chihara, Y. Fukata, M. Nakafuku, B. Yamamori, J. Feng, T. Nakano, K. Okawa, et al. 1996. Regulation of myosin phosphatase by Rho and Rho-associated kinase (Rho-kinase). *Science*. 273:245–248. http://dx.doi.org/10.1126/science.273.5272.245

Leung, T., X.Q. Chen, I. Tan, E. Manser, and L. Lim. 1998. Myotonic dystrophy kinase-related Cdc42-binding kinase acts as a Cdc42 effector in promoting cytoskeletal reorganization. *Mol. Cell. Biol.* 18:130–140.

Liao, X.H., J. Buggey, and A.R. Kimmel. 2010. Chemotactic activation of *Dictyostelium* AGC-family kinases AKT and PKBR1 requires separate but coordinated functions of PDK1 and TORC2. *J. Cell Sci.* 123:983–992. http://dx.doi.org/10.1242/jcs.064022

Limouze, J., A.F. Straight, T. Mitchison, and J.R. Sellers. 2004. Specificity of blebbistatin, an inhibitor of myosin II. *J. Muscle Res. Cell Motil.* 25:337–341. http://dx.doi.org/10.1007/s10974-004-6060-7

Liu, Y., J. Wang, M. Wu, W. Wan, R. Sun, D. Yang, X. Sun, D. Ma, G. Ying, and N. Zhang. 2009. Down-regulation of 3-phosphoinositide-dependent protein kinase-1 levels inhibits migration and experimental metastasis of human breast cancer cells. *Mol. Cancer Res.* 7:944–954. http://dx.doi.org/10.1158/1541-7786.MCR-08-0368

Maurer, M., T. Su, L.H. Saal, S. Koujak, B.D. Hopkins, C.R. Barkley, J. Wu, S. Nandula, B. Dutta, Y. Xie, et al. 2009. 3-Phosphoinositide-dependent kinase 1 potentiates upstream lesions on the phosphatidylinositol 3-kinase pathway in breast carcinoma. *Cancer Res.* 69:6299–6306. http://dx.doi.org/10.1158/0008-5472.CAN-09-0820

Merlot, S., and R.A. Firtel. 2003. Leading the way: Directional sensing through phosphatidylinositol 3-kinase and other signaling pathways. *J. Cell Sci.* 116:3471–3478. http://dx.doi.org/10.1242/jcs.00703

Miller, F.R., S.J. Santner, L. Tait, and P.J. Dawson. 2000. MCF10DCIS.com xenograft model of human comedo ductal carcinoma in situ. *J. Natl. Cancer Inst.* 92:1185–1186. http://dx.doi.org/10.1093/jnci/92.14.1185A

Najafov, A., E.M. Sommer, J.M. Axten, M.P. Deyoung, and D.R. Alessi. 2011. Characterization of GSK2334470, a novel and highly specific inhibitor of PDK1. *Biochem. J.* 433:357–369. http://dx.doi.org/10.1042/BJ20101732

Pearce, L.R., D. Komander, and D.R. Alessi. 2010. The nuts and bolts of AGC protein kinases. *Nat. Rev. Mol. Cell Biol.* 11:9–22. http://dx.doi.org/10.1038/nrm2822

Petrie, R.J., and K.M. Yamada. 2012. At the leading edge of three-dimensional cell migration. *J. Cell Sci.* 125:5917–5926. http://dx.doi.org/10.1242/jcs.093732

Petrie, R.J., N. Gavara, R.S. Chadwick, and K.M. Yamada. 2012. Nonpolarized signaling reveals two distinct modes of 3D cell migration. *J. Cell Biol.* 197:439–455. http://dx.doi.org/10.1083/jcb.201201124

Pinner, S., and E. Sahai. 2008. PDK1 regulates cancer cell motility by antagonising inhibition of ROCK1 by RhoE. *Nat. Cell Biol.* 10:127–137. http://dx.doi.org/10.1038/ncb1675

Ponti, A., M. Machacek, S.L. Gupton, C.M. Waterman-Storer, and G. Danuser. 2004. Two distinct actin networks drive the protrusion of migrating cells. *Science*. 305:1782–1786. http://dx.doi.org/10.1126/science.1100533

Price, J.T., T. Tiganis, A. Agarwal, D. Djakiew, and E.W. Thompson. 1999. Epidermal growth factor promotes MDA-MB-231 breast cancer cell migration through a phosphatidylinositol 3′-kinase and phospholipase C-dependent mechanism. *Cancer Res.* 59:5475–5478.

Primo, L., L. di Blasio, C. Roca, S. Droetto, R. Piva, B. Schaffhausen, and F. Bussolino. 2007. Essential role of PDK1 in regulating endothelial cell migration. *J. Cell Biol.* 176:1035–1047. http://dx.doi.org/10.1083/jcb.200607053

Primo, L., G. Seano, C. Roca, F. Maione, P.A. Gagliardi, R. Sessa, M. Martinelli, E. Giraudo, L. di Blasio, and F. Bussolino. 2010. Increased expression of alpha6 integrin in endothelial cells unveils a proangiogenic role for basement membrane. *Cancer Res.* 70:5759–5769. http://dx.doi.org/10.1158/0008-5472.CAN-10-0507

Raimondi, C., A. Chikh, A.P. Wheeler, T. Maffucci, and M. Falasca. 2012. A novel regulatory mechanism links PLCγ1 to PDK1. *J. Cell Sci.* 125:3153–3163. http://dx.doi.org/10.1242/jcs.100511

Ridley, A.J. 2011. Life at the leading edge. *Cell*. 145:1012–1022. http://dx.doi.org/10.1016/j.cell.2011.06.010

Riedl, J., A.H. Crevenna, K. Kessenbrock, J.H. Yu, D. Neukirchen, M. Bista, F. Bradke, D. Jenne, T.A. Holak, Z. Werb, et al. 2008. Lifeact: a versatile marker to visualize F-actin. *Nat. Methods*. 5:605–607. http://dx.doi.org/10.1038/nmeth.1220

Roussos, E.T., J.S. Condeelis, and A. Patsialou. 2011. Chemotaxis in cancer. *Nat. Rev. Cancer*. 11:573–587. http://dx.doi.org/10.1038/nrc3078

Sarbassov, D.D., D.A. Guertin, S.M. Ali, and D.M. Sabatini. 2005. Phosphorylation and regulation of Akt/PKB by the rictor-mTOR complex. *Science*. 307:1098–1101. http://dx.doi.org/10.1126/science.1106148

Scortegagna, M., C. Ruller, Y. Feng, R. Lazova, H. Kluger, J.L. Li, S.K. De, R. Rickert, M. Pellecchia, M. Bosenberg, and Z.A. Ronai. 2013. Genetic inactivation or pharmacological inhibition of *Pdk1* delays development and inhibits metastasis of $Braf^{V600E}$*::*$Pten^{-/-}$ melanoma. *Oncogene*. In press. http://dx.doi.org/10.1038/onc.2013.383

Tan, I., C.H. Ng, L. Lim, and T. Leung. 2001a. Phosphorylation of a novel myosin binding subunit of protein phosphatase 1 reveals a conserved mechanism in the regulation of actin cytoskeleton. *J. Biol. Chem.* 276:21209–21216. http://dx.doi.org/10.1074/jbc.M102615200

Tan, I., K.T. Seow, L. Lim, and T. Leung. 2001b. Intermolecular and intramolecular interactions regulate catalytic activity of myotonic dystrophy kinase-related Cdc42-binding kinase alpha. *Mol. Cell. Biol.* 21:2767–2778. http://dx.doi.org/10.1128/MCB.21.8.2767-2778.2001

Tan, I., J. Yong, J.M. Dong, L. Lim, and T. Leung. 2008. A tripartite complex containing MRCK modulates lamellar actomyosin retrograde flow. *Cell*. 135:123–136. http://dx.doi.org/10.1016/j.cell.2008.09.018

Tan, I., J. Lai, J. Yong, S.F. Li, and T. Leung. 2011. Chelerythrine perturbs lamellar actomyosin filaments by selective inhibition of myotonic dystrophy kinase-related Cdc42-binding kinase. *FEBS Lett.* 585:1260–1268. http://dx.doi.org/10.1016/j.febslet.2011.03.054

Tian, X., G. Rusanescu, W. Hou, B. Schaffhausen, and L.A. Feig. 2002. PDK1 mediates growth factor-induced Ral-GEF activation by a kinase-independent mechanism. *EMBO J.* 21:1327–1338. http://dx.doi.org/10.1093/emboj/21.6.1327

Tkachenko, E., M. Sabouri-Ghomi, O. Pertz, C. Kim, E. Gutierrez, M. Machacek, A. Groisman, G. Danuser, and M.H. Ginsberg. 2011. Protein kinase A governs a RhoA-RhoGDI protrusion-retraction pacemaker in migrating cells. *Nat. Cell Biol.* 13:660–667. http://dx.doi.org/10.1038/ncb2231

Toker, A., and A.C. Newton. 2000. Cellular Signaling: Pivoting around PDK-1. *Cell*. 103:185–188. http://dx.doi.org/10.1016/S0092-8674(00)00110-0

Uehata, M., T. Ishizaki, H. Satoh, T. Ono, T. Kawahara, T. Morishita, H. Tamakawa, K. Yamagami, J. Inui, M. Maekawa, and S. Narumiya. 1997. Calcium sensitization of smooth muscle mediated by a Rho-associated protein kinase in hypertension. *Nature*. 389:990–994. http://dx.doi.org/10.1038/40187

Vicente-Manzanares, M., X. Ma, R.S. Adelstein, and A.R. Horwitz. 2009. Non-muscle myosin II takes centre stage in cell adhesion and migration. *Nat. Rev. Mol. Cell Biol.* 10:778–790. http://dx.doi.org/10.1038/nrm2786

Waugh, C., L. Sinclair, D. Finlay, J.R. Bayascas, and D. Cantrell. 2009. Phosphoinositide (3,4,5)-triphosphate binding to phosphoinositide-dependent kinase 1 regulates a protein kinase B/Akt signaling threshold that dictates T-cell migration, not proliferation. *Mol. Cell. Biol.* 29:5952–5962. http://dx.doi.org/10.1128/MCB.00585-09

Weber, D.S., Y. Taniyama, P. Rocic, P.N. Seshiah, M.A. Dechert, W.T. Gerthoffer, and K.K. Griendling. 2004. Phosphoinositide-dependent kinase 1 and p21-activated protein kinase mediate reactive oxygen species-dependent regulation of platelet-derived growth factor-induced smooth muscle cell migration. *Circ. Res.* 94:1219–1226. http://dx.doi.org/10.1161/01.RES.0000126848.54740.4A

Wilkinson, S., H.F. Paterson, and C.J. Marshall. 2005. Cdc42-MRCK and Rho-ROCK signalling cooperate in myosin phosphorylation and cell invasion. *Nat. Cell Biol.* 7:255–261. http://dx.doi.org/10.1038/ncb1230

Yagi, M., A. Kantarci, T. Iwata, K. Omori, S. Ayilavarapu, K. Ito, H. Hasturk, and T.E. Van Dyke. 2009. PDK1 regulates chemotaxis in human neutrophils. *J. Dent. Res.* 88:1119–1124. http://dx.doi.org/10.1177/0022034509349402

Yamaguchi, H., J. Wyckoff, and J. Condeelis. 2005. Cell migration in tumors. *Curr. Opin. Cell Biol.* 17:559–564. http://dx.doi.org/10.1016/j.ceb.2005.08.002

Zhao, Z.S., and E. Manser. 2005. PAK and other Rho-associated kinases—effectors with surprisingly diverse mechanisms of regulation. *Biochem. J.* 386:201–214. http://dx.doi.org/10.1042/BJ20041638